

AD-753 958

AD 753 958

Investigation of Solidification of High Strength Steel

Massachusetts Institute of Technology

AUGUST 1972

Distributed By:

NTIS

**National Technical Information Service
U. S. DEPARTMENT OF COMMERCE**

AD753958



AD

AMMRC CTR 72-6/1

INVESTIGATION OF SOLIDIFICATION OF HIGH STRENGTH STEEL

August 1972

by D.S. Gnanamuthu, M. Basaran, T.Z. Kattamis, R. Mehrabian
and M.C. Flemings

Department of Metallurgy and Materials Science
Massachusetts Institute of Technology
Cambridge, Massachusetts 02139

Interim Report Covering Contract Number DAAG46-68-C-0043

Approved for public release; distribution unlimited.

13 1973

NATIONAL TECHNICAL
INFORMATION SERVICE

Prepared for

ARMY MATERIALS AND MECHANICS RESEARCH CENTER
Watertown, Massachusetts 02172

82

A

✓

The findings in this report are not to be construed as an official Department of the Army position, unless so designated by other authorized documents.

Mention of any trade names or manufacturers in this report shall not be construed as advertising nor as an official indorsement or approval of such products or companies by the United States Government.

DISPOSITION INSTRUCTIONS

Destroy this report when it is no longer needed.
Do not return it to the originator.

Unclassified

Security Classification

DOCUMENT CONTROL DATA - R & D

(Security classification of title, body of abstract and indexing annotation must be entered when the overall report is classified)

1. ORIGINATING ACTIVITY (Corporate author) Massachusetts Institute of Technology Cambridge, Massachusetts 02139		2a. REPORT SECURITY CLASSIFICATION Unclassified	2b. GROUP
3. REPORT TITLE Investigation of Solidification of High Strength Steel			
4. DESCRIPTIVE NOTES (Type of report and inclusive dates) Interim Report January 1, 1971 to December 31, 1971			
5. AUTHOR(S) (First name, middle initial, last name) Q D.S. Gnanamuthu, M. Basaran, T.Z. Kattamis, R. Mehrabian, and M.C. Flemings			
6. REPORT DATE August 1972	7a. TOTAL NO. OF PAGES 80	7b. NO. OF REFS 39	
8. CONTRACT OR GRANT NO. DAAG46-68-C-0043	9a. ORIGINATOR'S REPORT NUMBER(S) AMMRC CTR 72-6/1		
9. PROJECT NO. D/A IT062105A328	9b. OTHER REPORT NO(S) (Any other numbers that may be assigned this report)		
10. Agency Acession No. DA 0A4696			
11. DISTRIBUTION STATEMENT Approved for public release; distribution unlimited			
12. SPONSORING MILITARY ACTIVITY Army Materials and Mechanics Research Center, Watertown, Mass. 02172			
13. ABSTRACT Hot isostatic pressing of AISI 4340 low alloy steel was found to substantially accelerate micropore elimination. After a 30 hr. heat-treatment at 1315°C the remaining volume percent microporosity is 4×10^{-3} ; hot isostatic pressing of 1 hr. at 1260°C and 29,000 psi has completely eliminated microporosity. The study of the effect of homogenization on sulfides continued; Types I, II, III, and IV sulfides and sheet-like FeS inclusions coarsen during the treatment and finally become faceted. Ingots of the same steel containing 0.1% sulfur were unidirectionally solidified. The volume percent sulfides and the number of inclusions per unit volume of matrix slightly decreased with distance from the chill, whereas their mean overall size increased. During vacuum homogenization of cast material at 1315°C the volume percent sulfides remained practically unchanged, whereas their morphology changed to faceted. The number of inclusions per unit volume of matrix and the sulfide-matrix interface area per unit volume of sulfide decreased with homogenization time, whereas the mean overall size of inclusions increased. A coarsening model was introduced to describe coarsening kinetics. The time variation of the number of particles per unit volume exhibited a maximum, whereas that of the mean overall size minimum. These results are compatible with metallographic observations showing that the hot-rolled and elongated sulfide break-up into small segments which spheroidize with homogenization time and finally become faceted.			

Ia

DD FORM 1 NOV 64 1473

REPLACES DD FORM 1473, 1 JAN 64, WHICH IS
OBsolete FOR ARMY USE.

Unclassified

Security Classification

Unclassified

Security Classification

14. KEY WORDS	LINK A		LINK B		LINK C	
	ROLE	WT	ROLE	WT	ROLE	WT
Inclusions Morphology Homogenizing Solidification Microporosity Kinetics Low alloy steel						

I6

Security Classification

AMMRC CTR 72-6/1

INVESTIGATION OF SOLIDIFICATION OF HIGH STRENGTH STEEL

Technical Report by

D.S. Gnanamuthu, M. Basaran, T.Z. Kattamis, R. Mehrabian and M.C. Flemings

Massachusetts Institute of Technology
Cambridge, Massachusetts 02139

August 1972

Interim Report Contract Number DAAG46-68-C-0043

January 1, 1971 - December 31, 1971

D/A Project 1T062105A328

AMCMS Code 5025.11.294

Metals Research for Army Material

Agency Accession No. DA0A4696

Approved for public release; distribution unlimited.

Prepared for

ARMY MATERIALS AND MECHANICS RESEARCH CENTER
Watertown, Massachusetts 02172

IC

ABSTRACT

The effect of hot isostatic pressing of AISI 4340 low alloy steel on micropore elimination was investigated and was found to substantially accelerate it. After a 13 hr. heat-treatment at 1315°C the remaining volume percent microporosity is 5×10^{-3} after a 30 hr. treatment it is reduced to 4×10^{-3} ; hot isostatic pressing of 1 hr. at 1260°C and 29,000 psi has been found to completely eliminate microporosity. The study of the effect of homogenization on sulfides continued: Types I, II, III and IV sulfides and sheet-like FeS inclusions coarsen during the treatment and finally become faceted. Coarsening kinetics studies indicated that coarsening of Type II sulfides is probably controlled by the diffusion of sulfur.

Ingots ($2\frac{1}{4}$ inches x $3\frac{1}{4}$ inches x 6 inches) of AISI 4340 low alloy steel containing nominally 0.1% sulfur were unidirectionally solidified in a bottom-chilled exothermic mold. The volume percent sulfides and the number of inclusions per unit volume of matrix slightly decreased with distance from the chill, whereas their mean overall size increased. During vacuum homogenization of cast material at 1315°C the volume percent sulfides remained practically unchanged, whereas their morphology changed to faceted. The number of inclusions per unit volume of matrix and the sulfide-matrix interface area per unit volume of sulfide decreased with homogenization time, whereas the mean overall size of inclusions increased. A coarsening model was introduced to describe coarsening kinetics. During vacuum homogenization at 1315°C of rolled material there was practically no change in volume percent sulfides. The time variation of the number of particles per unit volume exhibited a maximum, whereas that of the mean overall size a minimum. These results are compatible with metallographic observations showing that the hot-rolled and elongated sulfides break-up into small segments which spheroidize with homogenization time and finally assume faceted forms.

TABLE OF CONTENTS

	<u>Page No.</u>
ABSTRACT	ii
FORWARD	iv
I. INTRODUCTION	1
II. EXPERIMENTAL PROCEDURE	7
Melting and Casting	
Homogenization Treatment and Hot Isostatic Pressing	
Thermomechanical Treatment	
Metallographic and Microradiographic Examination	
III. RESULTS	13
Effect of Hot Isostatic Pressing on Microporosity	
Effect of Homogenization on Structure of Sulfides	
Effect of Thermomechanical Processing on Sulfide Inclusion	
IV. DISCUSSION	19
Elimination of Microporosity by Hot Isostatic Pressing	
Morphological Changes of Sulfide Inclusions	
Changes in Size Distribution of Type II Sulfides	
Effect of Thermomechanical Processing on Sulfide Inclusions	
V. CONCLUSIONS	31
VI. REFERENCES	36

FOREWORD

This report was prepared by the Department of Metallurgy and Materials Science, Massachusetts Institute of Technology. The contract was administered under the technical supervision of Francis Quigley of the Army Materials and Mechanics Research Center, Watertown, Massachusetts.

I. INTRODUCTION

Results of studies on the effect of high temperature homogenization on sulfide inclusions and microporosity in unidirectionally solidified 4340 low alloy steel ingots were reported earlier¹. The ingot, prepared for studying the morphological modifications of sulfide inclusions, contained Type II, Type III, and a mixed Type II - III sulfides. It was found that during homogenization at 1315°C, for times between 20 and 100 hours Type II and mixed Type II - III sulfide inclusions coarsened and assumed compact polyhedral shapes. These shapes are expected to be less deleterious to mechanical properties than the original Type II and Type II - III inclusions.

Results of studies on the effect of homogenization on microporosity showed that its amount decreased with increasing homogenization time¹. Fine micropores near the chill disappeared faster than coarse micropores away from the chill. Nonspherical micropores gradually spheroidized during the treatment. The first part of the work reported herein is on the effect of homogenization, of unidirectionally solidified AISI 4340 low alloy steel, under high isostatic pressure (in excess of 20,000 psi) on volume percent and geometry of microporosity. Measurements were made using the microradiographic technique previously described¹.

The second part of this report contains results from our study of the effect of homogenization on the morphology of inclusions in unidirectionally solidified iron ingots containing a single type of sulfides. The composition of each ingot was controlled so that only a single type of sulfide formed during solidification. The types of sulfide inclusions whose morphological evolution during homogenization was studied were; Type I, Type II, Type III, Type IV and sheet-like FeS inclusions.

The third and major part of the work reported herein deals with the effect of thermomechanical processing of steel on sulfide inclusion volume percent, geometry, and distribution inside the steel matrix. The thermomechanical processing considered herein includes a combination of hot-rolling (heat-treatment and working) of slices taken from a columnar ingot and homogenization of the rolled product at various stages of the process.

Hot rolling or homogenization may be conducted at temperatures at which the inclusions are solid, partly liquid or entirely liquid. The anticipated effects of these treatments on inclusions may be summarized as follows:

1. Heat Treatment at a Temperature at Which Inclusions are Solid

This heat-treatment may affect the average composition of inclusions and the various phases which are present in them.

(a) Effect on Average Composition of Inclusions

In a study by Yarwood et al² on the formation of inclusions in the Fe-FeO-FeS system it was shown that large compositional differences exist between inclusions separated by very short distances. During heat-treatment oxygen and sulfur should be expected to diffuse in order to restore chemical equilibrium.

In a steel rich in sulfur and rapidly solidified the (Mn, Fe) S inclusions may have an Fe content higher than the equilibrium value and a Mn content lower than the equilibrium value. During heat-treatment one might anticipate that Mn would diffuse from the steel matrix to the sulfide phase and Fe would diffuse in the reverse direction, creating a Mn-depleted zone around the sulfide inclusion. In certain cases such zones have been observed by

Salmon Cox et³ and by Matsubara⁴.

These examples clearly indicate cases in which the average composition of inclusions could change during heat-treatment. Very limited quantitative information is available on this subject.

(b) Effect on Phases Present in Inclusions

It is well known that FeS precipitates, often in a Widmannstätten pattern, from a supersaturated (Mn, Fe)S phase solidified at steel-making temperature⁵. Spessartite and mullite (or even corundum) have been observed^{5,6} to precipitate from a glassy matrix in low-C steel deoxidized with Mn, Si and Al after a heat-treatment of 2 hours at 1100°C. Kiessling⁵ observed that dendritic cristobalite dispersed in Mn-silicate inclusions transformed to more stable tridymite during heat-treatment, whereas corundum transformed into galaxite. Again, besides these occasional observations no coherent study has been conducted on this problem.

2. Homogenization at a Temperature at Which Inclusions are Solid

Homogenization at a temperature at which inclusions are solid may affect their volume fraction, shape, size and distribution. Sims⁷ observed that sulfides spherodize after a heat-treatment of 24 hours at 1315°C. He also observed a very small dissolution of sulfides in resulfurized steel heat-treated at 1315°C; other authors^{6,8-11}, observed minor dissolutions of sulfides at temperatures above 1200°C. Gnanamuthu et al¹² conducted an extensive quantitative metallographic study of the effect of homogenization at 1315°C on sulfide inclusions in resulfurized AISI 4340 low alloy steel and observed that; (a) The total number of sulfide inclusions per unit volume

and the sulfide-matrix interface area per unit volume decreased with homogenization time, whereas the mean overall inclusion size increased and the volume fraction of sulfides remained practically unchanged; (b) For oxide and silicate inclusions none of these parameters changed in a measurable way with homogenization time; (c) Type I sulfides coarsened substantially with homogenization time and became faceted for longer times; Type II sulfides appearing in the ascast condition as an interdendritic eutectic network broke into segments which coarsened individually and ultimately became faceted for very long homogenization times. No quantitative information is yet available on the modifications of Type III sulfides. The spheroidization of sulfides and other nonmetallic inclusions was also observed by Hellner et al¹³ during homogenization of hot-rolled sheet of tool steel. This spheroidization was more significant in the case of small inclusions, as would have been expected. Similar observations were made by Vogels et al¹⁴.

3. Homogenization at a Temperature at Which Inclusions are Partly or Totally Liquid

Homogenization at a temperature at which inclusions are partly liquid would be expected to lead to coarsening (Ostwald Ripening)¹⁵⁻¹⁷ and coalescence of the solid part. Examples of such phenomena are occasionally mentioned in the literature¹⁸ but no quantitative study has yet been reported.

4. Hot-Rolling

Hot-rolling affects the geometry of inclusions in a way which depends directly on their deformability,¹⁹ that is their deformation relative to the

deformation of the steel matrix for different temperatures, pressures and velocities²⁰. Kiessling et al⁵ and Kiessling²¹ studied extensively the variation of the deformability of various inclusions (FeO, MnO, Al₂O₃, Ca-aluminates, spinel type double oxides, silicates and MnS) versus temperature.

The hardness of sulfide inclusions (Mn,Fe) S versus composition was investigated by Chao et al²². Chao et al^{23,24} investigated the relationship between plastic deformation of MnS in steel and the inclusions orientation and working temperature of the metal. Steel and MnS inclusions were found to exhibit sufficiently comparable deformation characteristics so that slip which initiated in steel continued through the inclusions and back into steel again, provided, of course, the inclusions orientation was favorable.

During hot-rolling softer phases deform plastically, whereas harder phases break up into strings of small crystals in the direction of deformation of the steel matrix⁵. Often hard inclusions, such as corundum, separate from a softer phase, such as aluminosilicate matrix, during rolling⁵. Pickering²⁵ studied the deformation and deformation and dissemination of nonmetallic inclusions during rolling and concluded that: (a) Fracture of the inclusions is necessary in order to disperse the larger detrimental inclusions into smaller, less harmful particles. (b) Fracture occurs at low deformation temperature or large hot-working reductions; larger inclusions fracture first. (c) Multiple hot-working with intermediate reheatings would seem preferable to all the hot-working being carried out with only one reheating. Hence, it is advisable to break down the larger injurious inclusions into less harmful dispersions by promoting an early fracture during the deformation process, perhaps by a low temperature working treatment. These particles are stress raisers and can be plastically deformed during

hot rolling.

Several of the effects previously summarized, of heat-treatment on inclusions, are also observed during hot-rolling. Thus, there are indications that the composition of sulfides changes during hot-rolling²⁶ and that phase transformations⁵ can occur faster during hot-rolling than during an ordinary heat-treatment. Coarsening during homogenization following hot-rolling and fragmentation of certain inclusions is expected to be faster because of the higher curvatures corresponding to finer particles. This expectation is justified by observations made by Hellner et al¹³.

To summarize: The intrinsic properties of the inclusions in steel, hence their composition and internal microstructure as compared with those of the matrix, their geometry and orientation with respect to the matrix control their behavior during thermomechanical processing and are expected to affect significantly the properties of the finished sheet; these characteristics vary during thermomechanical processing. A significant amount of useful information on the effect of thermomechanical processing on inclusions in steel still remains to be derived. It is the purpose of the work reported herein and of the work now in progress to contribute to a deeper understanding of this field.

II. EXPERIMENTAL PROCEDURE

Melting and Casting

Unidirectional ingots of 4340 low alloy steel and iron containing carbon, sulfur, and manganese were cast using equipment, and melting and casting procedures previously described.¹ Composition of the iron ingots was varied such that each ingot contained a single type of sulfide inclusions (Type I, Type II, Type III, Type IV, and sheet-like FeS inclusions). The starting material was high purity iron, Ferrovac E (99.9% pure), and the necessary amount of Fe-C master alloy. Approximately 700 grams of the alloy were melted in an alumina crucible under 1/2 atmosphere inert gas pressure. Additions of sulfur and manganese, as master alloys, were made 2 to 3 minutes prior to casting. The pouring temperature was between 1600 and 1650°C.

Each unidirectional ingot cast was approximately 2 inches high x 2 inches wide x 1.5 inches deep. Figure 1 is a schematic diagram of the chill and mold arrangement. Table I shows the compositions and types of inclusions in the unidirectionally solidified iron ingots.

The AISI 4340 low alloy steel used for investigating the effect of thermomechanical processing on inclusions was air-melted in an induction furnace with a 30KW, 10KC power supply, following a standard melting practice. The sulfur level in this material was brought up to 0.1 weight percent by addition of the appropriate amount of FeS, assumed stoichiometric, in order to follow easily the evolution of inclusions during their thermomechanical history.

The melt was cast and unidirectionally solidified in a composite mold supported by a water-cooled copper chill as shown schematically in Figure 2. The angle of the tapered exothermic sleeve in this mold was calculated as previously described²⁷. The space between the exothermic material and the stainless steel casting was filled with sodium silicate-bonded silica sand (CO₂-sand). Each ingot was approximately 6 inches high x 2.25 inches wide x 3.25 inches long.

Homogenization Treatment and Hot Isostatic Pressing

Specimens (1.0 cm x 1.0 cm x 4.0 cm) were taken from each 4340 ingot for high temperature, high pressure homogenization treatments. The hot isostatic pressing was carried out at 1250°C and 1038°C at pressures of 29,000 and 27,000 psi, respectively, using an ASEA press at Industrial Materials Technology, Inc. The samples were cold pressurized up to 13,000 psi, then heated to the desired temperatures at 900°F/hr. Pressurization was done using argon gas. In the homogenization treatment studies of sulfide inclusions, specimens were removed from each iron ingot at 2.5 cm from the chill and homogenized in vacuum (5×10^{-5} mm Hg) using an MRC vacuum furnace with tantalum heating elements. The homogenization treatments were carried out at temperatures between 950°C and 1315°C for times between 5 and 150 hours. At the end of each homogenization treatment, the power was shut off and the samples furnace-cooled.

Thermomechanical Treatment

The ingots made for studying the effect of thermomechanical processing on inclusions were sliced transversely and four slices were taken at 0.505,

1.54, 2.8 and 4.2 inches from the chill. These slices were hot-rolled at 1200°C in a Fenn 3F rolling mill. Several passes were made until reduction of 70 percent (3.3/l) and 85 percent (6.6/l) were obtained. In order to avoid any substantial cooling of the slices during rolling they were "sandwiched" using 1/4 inch thick low C steel sheet. This "pack-rolling" was interrupted by intermediate reheatings in a Lucifer furnace. Specimens for metallographic examinations were taken from the as-cast and from rolled material homogenized in vacuum at 1315°C for 0, 20, 50 and 100 hours. The specimens examined and their thermomechanical treatment are summarized in Table II.

Metallographic and Microradiographic Examination

For the study of the effect of homogenization on sulfide inclusions samples were taken at 2.5cm from the chill. They were ground and polished on diamond wheels and examined unetched using metallographic techniques. Detailed quantitative calculations of volume percent, size distribution, and matrix-sulfide interfacial area were carried out on sulfides as a function of homogenization time. The quantitative metallographic procedure and details of calculations were described previously ¹. Calculations were made for the sulfides assumed to be spherical in shape. The computer program, written in Fortran IV language for an IBM 360 System, was used for the foregoing calculations.

Microradiographic examination of microporosity was carried out on samples 0.005 cm thick removed from the as-cast, homogenized, and hot isostatically pressed material. The details of the X-ray apparatus, sample holder, and procedure employed to determine volume fraction and size distribution of the

micropores were previously described ¹.

The ingots prepared first for thermomechanical studies were first longitudinally polished and macroetched with a hydrochloric solution of FeCl_3 and CuCl_2 to determine the extent of columnar growth. On the average the columnar structure extended up to 85 percent of the ingot height. The various specimens processed thermomechanically, Table II, were ground, polished on diamond wheels and on a Syntron polisher and examined unetched. Quantitative metallographic techniques were used to evaluate the volume percent and average number of sulfides per unit volume of matrix, the mean overall size of inclusions and the sulfide-matrix interface area per unit volume of sulfide. Details of procedures used for these evaluation were given previously ¹. These procedures may be summarized as follows:

1. Measurement of Volume Percent Sulfides:

A two dimensional systematic point count procedure was used based on a coarse-mesh lattice criterion ²⁸. The samples were examined at 1000X using a 10 x 10 grid having 100 intersections. A total of 16000 points were projected. The volume percent was measured using the relationship

$$V = \frac{N_p}{N} \times 100 \quad [1]$$

where N_p = number of grid intersections falling on inclusions.

N = Total number of intersections projected.

Measurements were conducted directly on the screen of the metallograph using randomly chosen areas of the specimen. Similar measurements were also conducted using a Quantimet 720 computerized image analyzer. Discrepancies

between the results and those obtained by point-counting were substantial, probably because the contrast between inclusions and matrix is not very high and because of the existence of other types of inclusions. More confidence was, therefore, put on results obtained by point-counting.

For evaluating the other parameters by quantitative metallography it appeared necessary to apply Dehoff's modification ²⁹ of Saltykov's analysis by introducing a shape factor to correct for the nonequiaxed shape of inclusions, especially in the hot-rolled condition. However, it soon became evident that the assumption ²⁹ that inclusions could be assimilated with prolate or oblate ellipsoids of revolutions of constant axial ratio was far from realistic. In the hot-rolled condition it could be assumed that inclusions are in-between oblate and prolate ellipsoids of variable axial ratios. Thus, several classes of inclusions were defined per specimen, on the basis of their axial ration. The Number of Inclusions, N_j , in the j^{th} Class Per Unit Volume was determined by polishing down the specimen and counting inclusions in a given area, marked adequately with a microhardness tester, over a known thickness.

2. Measurement of the Total Sulfide-Matrix Interface Area per Unit Volume of Sulfide:

The total sulfide-matrix surface area per unit volume of matrix, S , is given ²⁹ by:

$$S = \sum_{j=1}^k N_j \left[\frac{\pi (A_j)^2}{2} + \frac{\pi (B_j)^2}{4E} \cdot \ln \left(\frac{1+E}{1-E} \right) \right] \text{ for an oblate ellipsoid.} \quad [2]$$

and

$$S = \sum_{j=1}^k N_j \left[\frac{\pi (B_j)^2}{2} + \frac{\pi (A_j)(B_j)}{2E} \sin^{-1} E \right] \text{ for a prolate ellipsoid.} \quad [3]$$

where: A_j = mean major axis

B_j = mean minor axis

$$E = \sqrt{\frac{(A_j)^2 - (B_j)^2}{A_j}}, \text{ excentricity} \quad [4]$$

N_j = number of inclusions in the j^{th} class per unit volume.

k = number of classes of inclusions having approximately the same shape, hence the same axial ration B_j/A_j and the same E .

S = sulfide-matrix interface area per unit volume of matrix.

The sulfide-matrix interface area per unit volume of sulfide, S_v , is related to S by the expression:

$$S_v = S/V$$

where V = volume percent of sulfide

3. Measurement of Mean Overall Size of Inclusions:

The mean overall size of inclusions, \bar{R} was determined by the following expressions:

$$R_j = \frac{2A_j + B_j}{6} \text{ for an oblate ellipsoid} \quad [5]$$

$$R_j = \frac{A_j + 2B_j}{6} \text{ for a prolate ellipsoid} \quad [6]$$

$$\bar{R} = \frac{\sum_{j=1}^k N_j R_j}{\sum_{j=1}^k N_j} \quad [7]$$

where: R_j = mean overall size of inclusions, for the j^{th} class.

III. RESULTS

Effect of Hot-Isostatic Pressing on Microporosity

Measured volume percent microporosity versus distance from the chill, in a unidirectionally cast 4340 low alloy steel ingot, in the as-cast homogenized, and hot isostatically pressed conditions is plotted in Figure 3. A specimen located 3cm away from the chill contains 2×10^{-2} volume percent microporosity. After homogenization treatment for 30 hours at 1315°C microporosity is reduced to 1×10^{-2} volume percent. No microporosity was observed in the same specimen hot isostatically pressed for 1 hour at 1260°C and 29,000 psi. Figure 4 shows microradiographs of the observed microporosity in the as-cast, homogenized, and hot isostatically pressed specimens.

Sections of another unidirectionally cast 4340 low alloy steel ingot were also hot isostatically pressed for 1 hour at 1260°C under 29,000 psi pressure, and at 1038°C under 27,000 psi pressure, respectively. Figure 5 shows that even at the lower temperature, 1038°C , there was no observable microporosity left in the specimen.

Effect of Homogenization on Structure of Sulfides

The composition, type of sulfide inclusions obtained, and pouring temperature of each unidirectionally solidified iron ingot is summarized in Table I. Figures 6 to 11 show the effect of homogenization treatment on Type I, Type II, Type III, Type IV, and sheet-like FeS inclusions. During homogenization at 1315°C the Type I sulfides, which are spherical in the as-cast condition, coarsen into polyhedral shapes, Figure 6. Type II sulfides are finely dispersed along the interdendritic regions forming a eutectic network in the as-cast condition. During homogenization

treatment at 1315°C they break into segments which coarsen into large faceted sulfides, Figure 7. Type III sulfides do not undergo a marked change in morphology. During homogenization treatment at 1100°C Type III sulfide coarsen, and the sharp edges and corners which are characteristic of these sulfides become smoother, Figure 8. Type IV sulfides undergo some changes in their morphology. During homogenization treatment at 1100°C Type IV sulfides coarsen, and become spheroidal, Figure 9. After long homogenization of 150 hours, some of the Type IV sulfides assume a faceted morphology. During this coarsening, dissolution takes place at the dendritic roots of these sulfides, Figure 10, with reprecipitation on the lateral surface of the arms.

Sheet-like FeS sulfide inclusions breakup during homogenization treatment at 955°C. They form angular or spheroidal inclusions at junctions between three or more grain boundaries. These inclusions coarsen by shortening and thickening, Figure 11.

The measurements on the distribution of Type II sulfides were made on samples taken at 2.5cm from the chill in ingot #2. The sulfides were extremely fine and in the polished section appeared either as beads or rods in the as-cast condition. After homogenization these sulfides assumed polyhedral shapes, Figure 7. The size distribution measurements were made assuming that the sulfides possess a spherical morphology.

The decrease in the total number of inclusions per unit volume during homogenization treatment at 1315°C is illustrated in Figure 12. The corresponding increase in the mean overall size of sulfide inclusions is shown in Figure 13. The size distribution as a function of homogenization treatment time is plotted in Figure 14. This figure clearly illustrates the decrease in the number of small sulfides and the corresponding increase in the number of large sulfides.

During homogenization the volume percent of sulfide inclusions remained unchanged, Figure 15, while the matrix-sulfide interfacial area decreased considerably, Figure 16.

The results reported above are also shown in tabulated form in Table III.

Effect of Thermomechanical Processing on Sulfide Inclusions

The morphology of sulfide inclusions at various stages of the thermomechanical treatment is illustrated in Figures 17-20. Metallographic studies on these inclusions may be summarized as follows:

1. Shape of Sulfide Inclusions:

In the as-cast condition inclusions are basically of Types II and III. During homogenization of the cast material there is a gradual break-up of Type II inclusions and formation of a new generation of faceted inclusions, called herein "Type III" inclusions. Both generations of Type III inclusions (the as-cast and those originating from geometric transformations of Type II inclusions during homogenization) coarsen substantially with increasing homogenization time.

In the as-rolled condition there are substantial variations in inclusion morphology, Figures 17 and 18, indicating variations in their deformability¹⁸, that is their deformation relatively to the deformation of the steel matrix.

In the rolled-and-homogenized condition it is generally observed that plastically deformed and elongated inclusions break into segments which spheroidize with homogenization time and become ultimately faceted, Figure 19. With increasing homogenization time the faceted sulfides coarsen further preserving their idiomorphic shape.

2. Volume Percent of Sulfide Inclusions:

The volume percent of sulfides (Types II and III) is plotted in Figure 21 versus distance from the chill for the as-cast condition and for the cast-and-homogenized condition at 1315°C for 20, 50 and 100 hours. It can be seen that: 1) the volume percent of sulfides increases in the proximity of the chill; 2) There is no measurable change in the volume percent of sulfides with homogenization time. Figure 22 shows that the volume percent of Type III sulfides increases with homogenization time by an amount which is basically independent of location from the chill. A comparison of Figures 21 and 22 shows that for a homogenization treatment of 100 hours all the Type II inclusions have been transformed into Type III.

The volume percent sulfides versus distance from the chill is plotted in Figures 23 and 24 for the rolled condition corresponding to reductions of 70% and 85%, respectively. These figures include information pertinent to as-rolled material and to material rolled-and-homogenized at 1315°C for 20, 50 and 100 hours. The following observations can be made on the basis of these plots: 1) In the rolled material, as reasonably expected, the volume percent sulfides is higher next to the chill than away from it; 2) homogenization does not seem to appreciably modify the volume percent sulfides; 3) plastic deformations during hot-rolling does not seem to affect the volume percent sulfides. It is a fact that volume percents in the material reduced 85% appear lower than those in the case material. This could be attributed to some systematic error during measurements by point counting due to the fineness of inclusions in the highly reduced state and their significant difference in geometry from that in the cast material.

3. Number of Sulfide Inclusions Per Unit Volume of Matrix:

The variation of the number of sulfides per unit volume of matrix, N , versus homogenization time is plotted in Figure 25 for cast specimens taken at different distances from the chill. It can be seen that in the as-cast condition this number is higher next to the chill and decreases with distance from the chill. Also, for shorter homogenization times up to 20 hours the rate of decrease of N with time is much higher near the chill than away from it. For longer homogenization times this difference in rates progressively decreases and becomes finally insignificant.

Figure 26 illustrates the variation of the N versus homogenization time for rolled material reduced 70%, with specimens taken at different distances from the chill. The striking observation which can be made is that there is an increase in N with increasing homogenization time followed by a gradual decrease analogous to that observed in Figure 25. The accurate position of the maximum is not known with the small number of specimens available. However, there is theoretical reason to believe that the homogenization time for which this maximum in N is reached increases with increasing distance from the chill. Another observation which can be made is that the rate of increase of N decreases with increasing distance from the chill. The same observation holds for the rate of decrease of N following the maximum on the curve.

Similar observations can be made on Figure 27 which illustrates the variation of N versus homogenization time for rolled material reduced 85% with specimens taken at various distances from the chill. The maxima in N attained in this case are higher than in the case of specimens reduced 70%, Figure 26.

Figures 25 and 27 have been combined for plotting Figure 28. In this graph N is plotted versus distance from the chill for cast material and rolled material

reduced 70% and 85% with specimens in the as-processed condition or homogenized for 50 hours. This graph emphasizes the fact that in all conditions N decreases with increasing distance from the chill. In the cast condition N is lower in the homogenized state, whereas in the rolled condition it is higher, especially for the material of higher reduction.

4. Mean Overall Size of Inclusions:

The variation of the mean overall size of sulfides versus homogenization time for cast specimens taken at different distances from the chill is given in Figure 29. The mean overall size of sulfides increases with homogenization time, this increase being faster for inclusions in the material close to the chill.

For rolled material the mean overall size of sulfides first decreases, reaches a minimum whose position is not known with accuracy, and subsequently increases, Figures 30 and 31. The mean overall size is larger for specimens taken away from the chill and for specimens reduced less during hot-rolling.

5. Sulfide-Matrix Interface Area Per Unit Volume of Sulfide:

The dependence of the sulfide-matrix interface area per unit volume of sulfide, S_v , on homogenization time is illustrated in Figure 32 for cast material and specimens taken at different distances from the chill. S_v decreases with homogenization time for specimens taken at a given distance from the chill and with distance from the chill for specimens homogenized for the same time. For short homogenization times the rate of decrease of S_v with time is higher for specimens taken from the vicinity of the chill. For long homogenization times the rate of decrease of S_v with time becomes almost independent of distance from the chill.

IV. DISCUSSION

Elimination of Microporosity by Hot Isostatic Pressing

The complete elimination of microporosity by hot isostatic pressing is illustrated in Figures 3 to 5. The elimination of micropores by diffusion of vacancies from pore surfaces to grain boundaries depends on the amount of porosity, pore size and distribution, grain size and interaction of grain boundaries with porosity. The following expression was developed by Flemings and Coble³⁰ for the elimination of a pore of size r_0 under an isostatic pressure:

$$\Delta t = \left(-\frac{kT}{2D_L \Omega \sigma} r^2 \right) \frac{r}{r_0} \quad [8]$$

or, because of complete pore elimination, $r = 0$ and

$$\Delta t = \frac{kT}{2D_L \Omega \sigma} r_0^2 \quad [9]$$

where Δt = heat treatment time to remove a pore of radius r_0 , sec.

k = Boltzmann's constant, ergs/ $^{\circ}$ Kx atom.

T = absolute heat-treatment temperature, $^{\circ}$ K.

D_L = lattice diffusion coefficient, cm^2/sec .

Ω = atomic volume, cm^3 .

σ = applied normal stress (pressure), dyn/cm^2 .

Values adopted for these parameters were:

$D_L = 3.2 \times 10^{-10} \text{ cm}^2/\text{sec}$, using data from reference 31.

$k = 10^{-16} \text{ ergs}/^{\circ}\text{Kx atom}$.

$T = 1533^{\circ}\text{K}$

$\Omega = 10^{-23} \text{ cm}^3/\text{atom}$.

$r_0 = 7 \times 10^{-4} \text{ cm}$.

It can be deduced from [9] that Δt is 98 min. for a pore radius of 7 microns. This is a maximum pore radius. On the average, a pore radius in the treated specimens is approximately 2.7 microns which would then necessitate 14 minutes for elimination. This is quite shorter than the experimentally measured time of 1 hour. It can then be concluded that the Coble et al³⁰ model describes the elimination of microporosity in a satisfactory way. One of the basic assumptions of the model is that there is one pore per grain, hence, that the interpore spacing is larger than the average grain size. This assumption is valid in the present case: Interpore spacing has been measured and found equal to 200 microns and grain size equal to 36 microns.

In order to decide whether the pores disappear through high temperature grain boundary sliding under the effect of pressure or through diffusion of vacancies to grain boundaries, the following calculation was made:

The internal pressure necessary to create a pore is given by the elasticity-plasticity theory as equal to:³²

$$p = \frac{2Y}{3} \left[1 + \ln \frac{2E}{3Y} \right] + \frac{2\pi^2 H'}{27} \quad [10]$$

where: p = tension, psi

Y = yield strength, psi

E = elastic, psi

H' = constant hardening rate

The same expression could logically be used to evaluate the pressure necessary to close-up a pore, by such a mechanism as grain-boundary sliding for example. The following values were adopted for low alloy steel at about 1250°C:

$$Y = 35,000 \text{ psi}$$

$$E = 21 \times 10^6 \text{ psi}$$

$$H' = 17,000 \text{ psi}$$

Therefore, $p = 175,000 \text{ psi}$ which is much higher than the pressure used during the present isostatic hot pressing. Thus, it can be concluded that the porosity could not possibly be eliminated by closing of pores under pressure through a mechanism such as grain boundary sliding. The most probable mechanism for this elimination is the diffusion of vacancies to grain boundaries.

Morphological Changes of Sulfide Inclusions

During homogenization all the different types of sulfide inclusions coarsen into fairly consistent polyhedral shapes. The homogenization times necessary to reach the polyhedral shape varies with the initial sulfide morphology, and homogenization temperature. For example, dendritic Type IV sulfides become polyhedral in shape after 150 hours at 1100°C , Figure 9, whereas Type I and II sulfides assume coarse polyhedral shapes after 40 to 50 hours at 1315°C , Figures 6 and 7, respectively. The observations on sheet-like FeS inclusions are in agreement with those of Keh and Van Vlack ³³.

Changes in Size Distribution of Type II Sulfides

Results from ingot #2, containing Type II sulfides reveal that during homogenization the average inclusion size increases with a parallel decrease in the number of small size sulfide inclusions, leading to a reduction in the total number of sulfide inclusions. The changes in size distribution are essentially due to coarsening whose driving force is the reduction in total sulfide-matrix interfacial energy.

Coarsening kinetics have been studied by Lifshitz et al³⁴, Wagner³⁵, Greenwood³⁶ and other authors, using diffusion models based on a variety of simplifying assumptions. Thus, for a diffusion-controlled process the mean particle diameter may be expressed by:

$$\bar{d}^3 - \bar{d}_0^3 = Kt = \frac{64}{9} \frac{\gamma CVD}{vRT} \bar{V}^2 t \quad [11]$$

where: \bar{d} = mean diameter of inclusion at time t

\bar{d}_0 = mean diameter of inclusion at time zero

K = coarsening rate constant

γ = matrix-sulfide interfacial energy

C = equilibrium solubility of sulfur in the alloy

\bar{V} = molar volume of MnS

D = rate controlling diffusion coefficient

v = factor depending on the stoichiometry of MnS

R = gas constant

T = absolute temperature

A plot of $(\bar{d}^3 - \bar{d}_0^3)$ versus homogenization time is shown in Figure 33.

A linear relationship is obtained, thus indicating that coarsening of Type II sulfides is probably diffusion controlled. From this analysis it is not possible to determine whether the diffusion of manganese or that of sulfur is rate controlling. It is likely that the diffusion of sulfur is rate-controlling despite its higher diffusivity³⁷, because of its lower solubility in iron. In fact, γ -iron at 1335°C dissolves no more than 0.046% sulfur³⁸, while the solubility of manganese at the same temperature is about³⁹ 40%.

Effect of Thermochemical Processing on Sulfide Inclusions

1. Shape of Sulfide Inclusions:

During homogenization of the cast material there is a gradual break-up

of Type II inclusions, spheroidization of the resulting segments and finally transformation of spheroids into faceted polyhedral forms. Such geometric changes have been reported earlier. The observed faceting of sulfide inclusions may be caused by one or more of the following factors:

- 1) Preferred crystallographic growth of the sulfide in certain directions;
- 2) at the homogenization temperature the sulfide inclusions and the matrix reach some kind of equilibrium shape which is preserved in the casting in spite of the martensitic transformation of the matrix.

In the as-rolled condition there is a variety of inclusion morphologies. Thus, it is observed that near the chill they are thin and elongated, whereas away from the chill they are thicker and shorter. Obviously near the chill plastic deformation of inclusions during hot-rolling has been more extensive than away from the chill. This could presumably be attributed to a variation in composition of inclusions depending on their position with respect to the chill. These conclusions cannot be confirmed with certainty because no microhardness measurements or electron microprobe analysis have yet been conducted on inclusions. Indeed, it is expected that electron microanalysis will establish the relative amounts of Mn, Fe and other elements in the sulfide solid solution [Mn, Fe, X] S versus distance from the chill.

The presence of hard oxide cores or silicates inside sulfide inclusions can drastically effect their deformation behavior during rolling. This is illustrated in Figures 18b and c, where the black spots inside the sulfides could be corundum (Al_2O_3) particles.

Type II sulfides deform more uniformly than Type III sulfides whose orientation with respect to the rolling plane and rolling direction can

often affect their final morphology after plastic deformation.

In the rolled-and-homogenized condition the elongated inclusions break into segments which gradually spheroidize and finally assume faceted forms, Figure 19. This mechanism is schematically illustrated in Figure 34.

2. Volume Percent of Sulfide Inclusions:

In the as-cast and in the rolled conditions it is observed that there is an increase in the volume percent of sulfides close to the chill. This increase could be attributed to some kind of inverse segregation or possibly to the nonequilibrium nature of solidification, due to higher cooling rates next to the chill.

The solubility of sulfur in the steel matrix is very limited,³⁸ hence during homogenization there can be no decrease in the amount of precipitated sulfide. This is exactly what is observed.

The gradual break-up and transformation of Type II sulfide inclusion into faceted "Type III" inclusions during homogenization of cast material is clearly illustrated in Figure 22.

3. Number of Sulfide Inclusions Per Unit Volume of Matrix:

The number of sulfide inclusions per unit volume of matrix decreases with homogenization time due to coarsening. It is known and will be repeated in a subsequent chapter that rate of coarsening increases with decreasing particle size. Hence, the observation made in Figure 25 that for shorter homogenization times the rate of coarsening is higher for inclusions close to the chill than for those situated away from the chill; inclusions close to the chill are finer, Figure 29.

In the rolled-and-homogenized condition there is an increase in N followed by a decrease after a certain maximum has been reached. This is in agreement with the observed break-up of elongated inclusions into segments and their subsequent spheroidization and faceting. The maximum in N is higher for inclusions in specimens close to the chill, presumably because after deformation these inclusions are thinner and longer and can break into a larger number of segments.

4. Distribution of Inclusions:

In the as-rolled condition the fine elongated sulfide inclusions, observed in specimens taken near the chill, are fairly randomly distributed in the steel matrix, Figure 17a. In specimens taken away from the chill sulfide inclusions are distributed in groups, Figure 17b. This could be attributed to the coarseness of dendrites in these specimens. After plastic deformation of these specimens inclusions which are interdendritic would tend to group together.

In the rolled-and-homogenized condition faceted sulfide inclusions tend to be grouped in lines in specimens taken near the chill. They tend to be randomly distributed in specimens taken away from the chill. This again could be explained on the basis of the break-up-spheroidization-faceting mechanism described above.

5. Mean Overall Size Inclusions:

The mean overall size of sulfide inclusions increases with homogenization time due to coarsening. Figure 29 which is faster for finer inclusions in specimens taken close to the chill.

The minimum in mean overall size observed in specimens which were

rolled-and-homogenized should be explained again on the basis of the break-up-spheroidization-faceting mechanism. Beyond this minimum coarsening is responsible for the gradual increase in mean overall size of inclusions.

6. Sulfide-Matrix Interface Area Per Unit Volume of Sulfide:

The coarsening of inclusions in the cast condition is responsible for the observed decrease in S_v with homogenization time. Experimental study of the time variations of S_v in rolled material has not yet been completed, however, it is anticipated that S_v would decrease; the break up of elongated inclusions into smaller does not necessarily imply an increase in S_v .

In order to more fully understand the operation of coarsening, a coarsening model will be developed herein to describe coarsening kinetics of sulfide inclusions during isothermal homogenization of steel. Coarsening kinetics will be expressed as a time variation of the sulfide-matrix interface area per unit volume of sulfide, S_v , and of the number of inclusions per unit volume, N .

Assume a system of N spherical inclusions of radii $R_1, R_2, \dots, R_1, \dots, R_n$. The assumption of sphericity limits this analysis to cast material only.

The general expression for the rate of change of the radius of a sphere during coarsening may be written as:³⁶

$$\frac{dR_1}{dt} = \frac{2DM\sigma S}{RTR_{10}^2} \left(\frac{1}{R} - \frac{1}{R_1} \right) \quad [12]$$

where D = diffusivity of solute in the solid, $\text{mm}^2/\text{sec.}$

M = molecular weight, gm/mole.

σ = particle-matrix interface energy, cal/mm^2

S = solubility of solute in the matrix, gm/mm³

R = gas constant, cal/mole x°K

T = absolute temperature, °K

R_i = radius of i^{th} particle, mm

\bar{R} = average radius of the particle population, mm

ρ = density of sulfide, gm/mm³

The radius of the sphere i , R_i , may be expressed versus time by:

$$R_i = R_{i0} + \int_0^t \frac{dR_i}{dt} dt \quad [13]$$

where R_{i0} = the initial radius of the i^{th} particle, mm.

t = time, sec.

Hence, from [12] and [13]:

$$R_i = R_{i0} + \int_0^t \frac{2DM\sigma S}{RTR_i} \left(\frac{1}{R} - \frac{1}{R_i} \right) dt \quad [14]$$

where : R_i and \bar{R} are functions of time and all the other factors are constant for an isothermal treatment.

Expression [13] may be approximated by:

$$R_i(t) = R_{i0} + \lim_{\Delta t \rightarrow 0} \sum_{k=0}^{t_k} \frac{dR_i}{dt} \cdot \Delta t_k \quad [15]$$

where: $\frac{dR_i}{dt} \cdot \Delta t_k = \frac{dR_i}{dt}$ calculated at the beginning of the k^{th} time step

Δt_k = length of k^{th} time step, sec.

$R_i(t)$ = radius of the i^{th} particle at the end of the k^{th} time step.

From [12] and [15]:

$$R_i(t) = R_{i0} + \lim_{k \rightarrow \infty} \sum_{t=0}^{t_k} \frac{2DMoS}{RTR_{ik}} \left[\frac{1}{R_k} - \frac{1}{R_{ik}} \right] \Delta t_k \quad [16]$$

where: \bar{R}_k , R_{ik} = average radius of the population and radius of particle i , respectively, at the beginning of the k^{th} time step.

R_i at the beginning of the k^{th} time step has precisely the same value as at the end of the $(k-1)^{\text{th}}$ time step and the initial value of R_i , R_{i0} , is known. Thus, expression [16] can be evaluated by means of a digital computer. More specifically: A system of n inclusions is assumed at time $t = 0$, hence R_{i0} and \bar{R}_0 are known. At the end of the first step the new distribution of particle radii can be deduced from [16], hence a new \bar{R}_1 can be calculated and so forth.

The surface-to-volume ratio of the system of particles S_v , may be defined as:

$$S_v = \frac{\sum_{i=1}^n 4\pi r_i^3}{\sum_{i=1}^n \frac{4\pi r_i^3}{3}} \quad [17]$$

At time $t = \sum_{k=1}^k t_k$, $S_v(t)$ is given by:

$$S_v(t) = \frac{s(t)}{s(0)} \quad S_v(0) \quad [18]$$

Where S_v = surface area per unit volume of inclusions, mm^{-1}

S = total surface of particles in the system.

Expression [18] is justified by the constance of volume of sulfides during isothermal coarsening.

The number of particles versus volume is given by:

$$N(t) = \frac{n(t)}{n(o)} N(o)$$

where: $N(t)$ = number of particles per unit volume at time t

$N(o)$ = number of particles per unit volume at time o

n = total number of particles in the system.

Metallographic examination of successive surfaces obtained by polishing down a specimen taken at 0.50 inches from the chill has shown that a typical size distribution would be the following:

<u>Number of Particles</u>	<u>Radius, mm</u>
5	0.005
5	0.0010
2	0.0015
1	0.0020
1	0.0025
1	0.0030
1	0.0035
1	0.0045
1	0.0055
1	0.0070

This distribution has been taken as initial distribution in this coarsening analysis. The various parameters in expression [16] were

attributed the following values $\sigma = 1.20 \times 10^{-7}$ cal/mm², $M = 87$ gm/mole
 $R = 2$ cal/mole. $^{\circ}$ K, $\rho = 3.99 \times 10^{-3}$ gm/mm³, $S = 0.003$ gms/100 gms of steel =
 0.234×10^{-6} gm/mm³, $T = 1588^{\circ}$ K and $D = 7.5 \times 10^{-6}$ mm²/sec.

Figure 35 illustrates the analytical curve thus obtained. This curve does not coincide with the experimental curve corresponding to five inclusions taken next to the chill. The discrepancy is, nonetheless acceptable, owing to the uncertainty of certain values of the parameters used and to the assumptions on which the model was based.

V. CONCLUSIONS

1. Hot isostatic pressing of AISI 4340 low alloy steel was found to substantially accelerate micropore elimination. Thus, after a 13 hr heat-treatment at 1315°C the remaining volume percent microporosity is 0.005, after a 30 hr treatment it is reduced to 0.004. After a 1 hr hot isostatic pressing at 1260°C and 29000 psi microporosity is completely eliminated.
2. Types I, II, III and IV sulfides and sheet-like FeS inclusions coarsen during homogenization treatment and finally assume compact polyhedral shapes.
3. Study of coarsening kinetics indicated that coarsening of Type II sulfides is probably controlled by the diffusion of sulfur.
4. In a unidirectionally solidified AISI 4340 low alloy steel ingot containing nominally 0.1% sulfur the volume percent sulfides and the number of sulfide particles per unit volume of matrix slightly decrease with distance from the chill, whereas their mean overall size increases. Also, their deformability decreases with distance of the chill presumably due to a compositional change.
5. During homogenization of cast material the volume percent sulfides remains practically unchanged, whereas their morphology changes: Type II inclusions break-up into segments which spheroidize and become finally faceted. Also, the numbers of inclusion per unit volume of matrix decreases and their mean overall size increases with homogenization time. A coarsening model was introduced assuming spherical inclusions and the variation of S_v with homogenization time was established. Analytical predictions and experimental measurements of S_v agree

reasonably well for short homogenization times up to about 50 hours.

6. During homogenization of rolled material there is practically no change in volume percent of sulfide. The number of sulfides per unit volume of matrix first increases, reaches a maximum and subsequently decreases with increasing homogenization time. The mean overall size of inclusions first decreases, reaches a minimum beyond which it increases with increasing homogenization time. These results are compatible with metallographic observations showing that the plastically deformed, elongated sulfides break-up into small segments which spheroidize with homogenization time and finally assume faceted forms.

TABLE I
CHEMICAL ANALYSIS OF IRON INGOTS
(Weight Percent)

Ingot Number	S	O	C	Al	Si	Mn	Pouring Temperature of Ingots (°C)	Sulfide Type
1 0.096	0.0052	0.0079	NA	<0.01	0.90	1650		I
2 0.26	0.0048	0.0096	0.13	0.01	1.34	1650		II
3 0.10	0.017	2.63	NA	0.03	2.58	1640		III
4 0.27	0.014	2.99	NA	0.05	2.56	1640		IV
5 1.15	0.012	0.023	6.10	0.01	<0.01	1600	Sheet-like FeS	

NA: Not Analyzed

TABLE II
SUMMARY OF THERMOMECHANICAL PROCESSING

CONDITION OF MATERIAL			
HOMOGENIZATION TIME AT 1315°C	As-cast	Reduced 70%	Reduced 85%
	Specimen I*	Specimen I	Specimen I
	II	II	II
	III	III	III
	IV	IV	IV
20 HRS.	Specimen I	Specimen I	Specimen I
	II	II	II
	III	III	III
	IV	IV	IV
50 HRS.	Specimen I	Specimen I	Specimen I
	II	II	II
	III	III	III
	IV	IV	IV
100 HRS.	Specimen I	Specimen I	Specimen I
	II	II	II
	III	III	III
	IV	IV	IV

*Specimen I was taken 0.505 inches from the chill

Specimen II was taken 1.54 inches from the chill

Specimen III was taken 2.8 inches from the chill

Specimen IV was taken 4.2 inches from the chill

TABLE III
RESULTS FOR TYPE II SULFIDES LOCATED AT 2.5 cm
FROM CHILL IN INGOT #2

Homogenization Treatment at 1315°C Time (hours)	Volume Percent	Surface Area (cm ² /cm ³)	Number per cm ³	Mean Radius (microns)
0	1.53 ± 0.23	786 ± 140	1.5 x 10 ¹⁰	0.43
5	1.57 ± 0.23	352 ± 69	1.9 x 10 ⁹	0.82
10	1.55 ± 0.23	240 ± 41	4.3 x 10 ⁸	1.29
20. 25	1.53 ± 0.23	171 ± 38	1.9 x 10 ⁸	1.62
40	1.52 ± 0.23	104 ± 43	8.6 x 10 ⁷	2.07

REFERENCES

1. D. S. Gnanamuthu, M. Basaran, T. Z. Kattamis, R. Mehrabian and M. C. Flemings, "Investigation of Solidification of High Strength Steel," M.I.T., Contract No. DAAG46-68-C-0043, Army Materials and Mechanics Research Center, CTR 72-1, Interim Report, January 1 - December 31, 1970.
2. J. C. Yarwood, M. C. Flemings and J. F. Elliott: Met. Trans., Vol. 2, 1971, pp. 2573-2582.
3. P. H. Salmon Cox and J. A. Charles: J.I.S.I., 1965, vol. 203, pp. 493-99.
4. K. Matsubara: "The Electron Microprobe", Proc. Symp. Electrochem. Soc., Washington, D. C., 1964, pp. 632-41.
5. R. Kiessling and N. Lange: "Non-Metallic Inclusions in Steel", Parts I-III, The Iron and Steel Institute Special Report 90 and Publications 100 and 115, London, 1964, 1966 and 1968.
6. P. J. H. Mauder and J. A. Charles: J.I.S.I., 1968, vol. 206, pp. 705-15.
7. C. E. Sims: Trans. AIME, 1959, vol. 215, pp. 367-93.
8. J. H. Andrew and D. Binnie: J.I.S.I., 1929, vol. 119, pp. 346-58.
9. E. Gregory and J. H. Whiteley: J.I.S.I., 1911, vol. 144, pp. 9-48.
10. K. J. Irvine: J.I.S.I., 1952, vol. 171, pp. 142-47.
11. T. Bonizewski and R. G. Baker: J.I.S.I., 1964, vol. 204, pp. 921-28.
12. D. Gnanamuthu, T. Z. Kattamis and M. C. Flemings: current investigation, Department of Metallurgy and Materials Science, M.I.T.
13. L. Hellner and T. O. Norrman: Jernkont. Ann., 1968, vol. 152, pp. 269-86.
14. J. A. Vogels, W. Dahl, H. Hengstenberg and F. Brünning: Arch. Eisenhütten., 1962, vol. 33, pp. 649-59.
15. T. Z. Kattamis, J. M. Coughlin and M. C. Flemings: Trans. AIME, 1967, vol. 239, pp. 1504-11.
16. T. Z. Kattamis, U. T. Holmberg and M. C. Flemings: J.I.S.I., 1967, vol. 95, pp. 343-47.
17. J. J. Reeves and T. Z. Kattamis: Scripta Met., 1971, vol. 5, pp. 223-29.
18. L. H. Van Vlack, O. K. Riegger, R. J. Warrick and J. M. Dahl: Trans. AIME, 1961, vol. 221, pp. 220-28.
19. T. Malkiewicz and S. Rundnik: J.I.S.I., 1963, vol. 201, pp. 33-38.
20. F. Garofalo, G. V. Smith and D. C. Madsen: Trans. ASM, 1957, vol. 49, p. 372.

21. R. Kiessling: J. of Met., October 1969, vol. 21, pp. 48-54.
22. H. Chao, L. H. Van Vlack, F. Oberin and L. Thomassen: Trans. ASM, 1964, vol. 57, pp. 885-91.
23. H. Chao and L. H. Van Vlack: Trans. AIME, 1965, vol. 233, pp. 1227-31.
24. H. C. Chao and L. H. Van Vlack: Trans. ASM, 1965, vol. 58, pp. 335-40.
25. F. B. Pickering: J.I.S.I., 1958, vol. 189, pp. 148-59.
26. S. Bergh: Jernkont. Ann., 1968, vol. 152, pp. 451-52.
27. G. E. Nereo, R. F. Polich and M. C. Flemings: Trans. AFS, 1965, vol. 73, pp. 1-13.
28. J. E. Hilliard and J. W. Cahn: Trans. AIME, 1961, vol. 221, pp. 344-52.
29. R. T. Dehoff: Trans. AIME, 1962, vol. 224, pp. 474-77.
30. R. L. Coble and M. C. Flemings: Met. Trans., vol. 2, 1971, pp. 409-415.
31. C. J. Smithells: Metals Reference Book, London, Butterworths, p. 644.
32. R. Hill: "The Mathematical Theory of Plasticity," Oxford Clarendon Press, 1960, p. 106.
33. A. S. Keh and L. H. Van Vlack: Trans. AIME, 1959, pp. 950-958.
34. I. M. Lifshitz and V. V. Slyozov: J. Phys. Chem. Solids, 19, 1961, pp. 35-50.
35. C. Wagner: Z. Electrochem., 65, 1961, pp. 581-591.
36. G. Greenwood: Acta Met., 4, 1956, pp. 243-248.
37. N. G. Ainslie and A. V. Seybolt: S.I.S.I., 1960, pp. 341-350.
38. E. T. Turkdogan, S. Ignatowicz and S. Pearson: S.I.S.I., vol. 180, 1955, pp. 349-354.
39. M. Hansen, "Constitution of Binary Alloys," McGraw-Hill Book Co., Inc., New York, 1958.

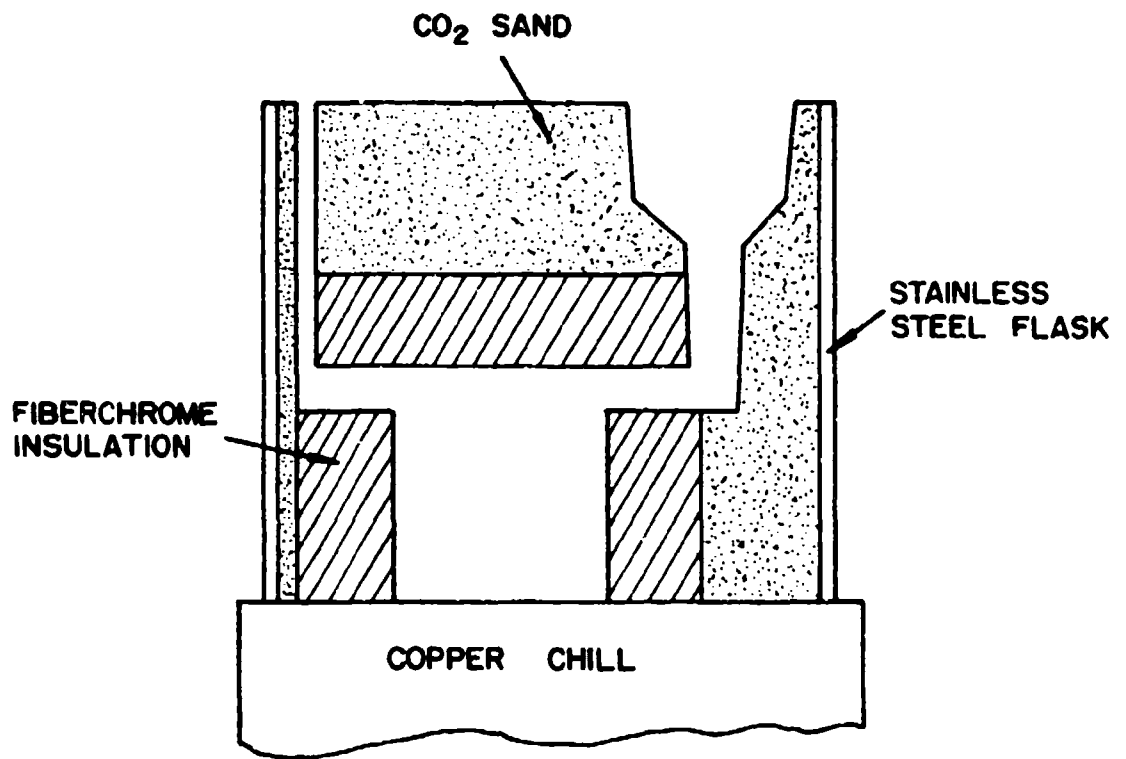


Figure 1. Schematic illustration of the Fiberchrome mold used.

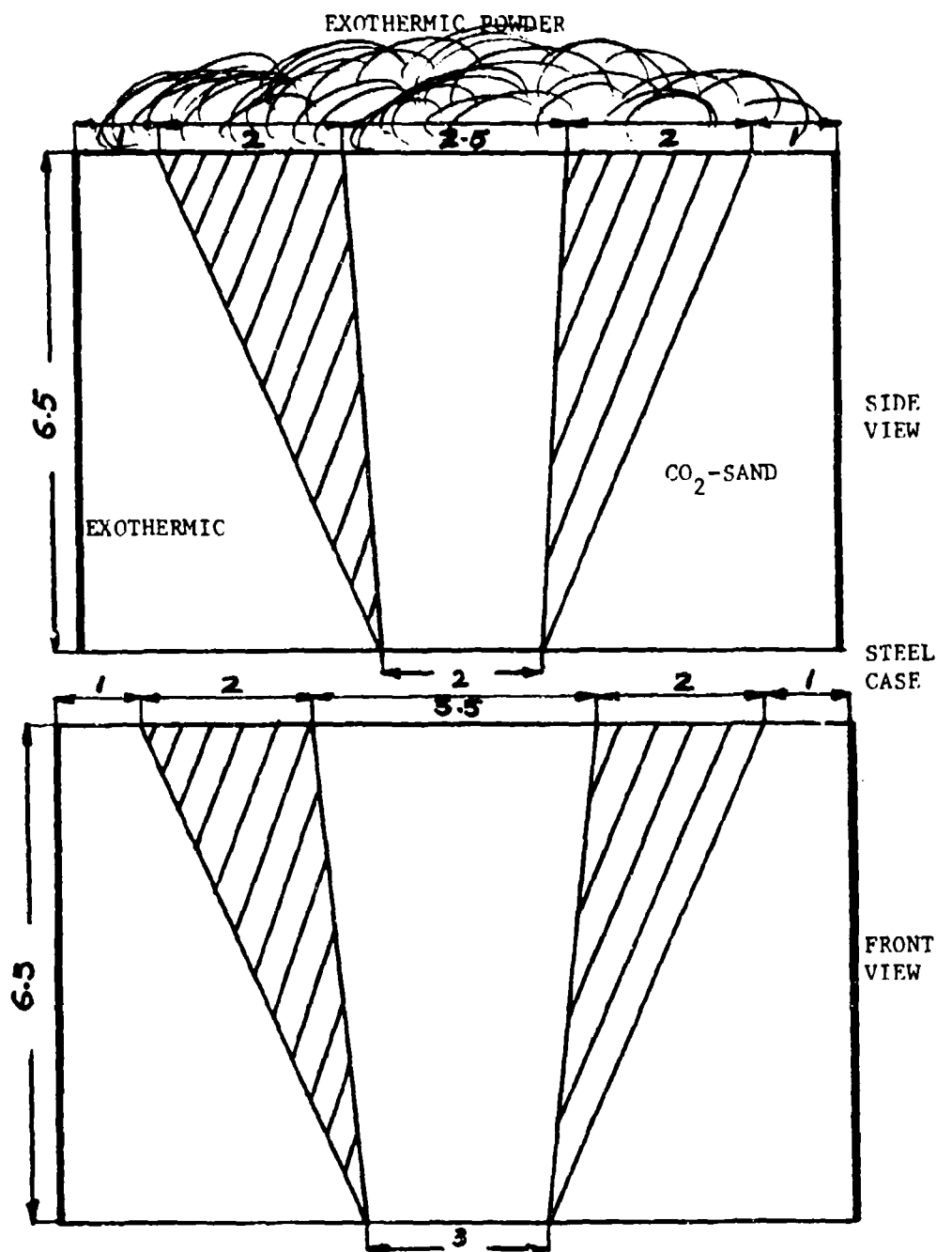


Figure 2: Mold used for unidirectional solidification of AISI 4340 steel. Dimensions are in inches.

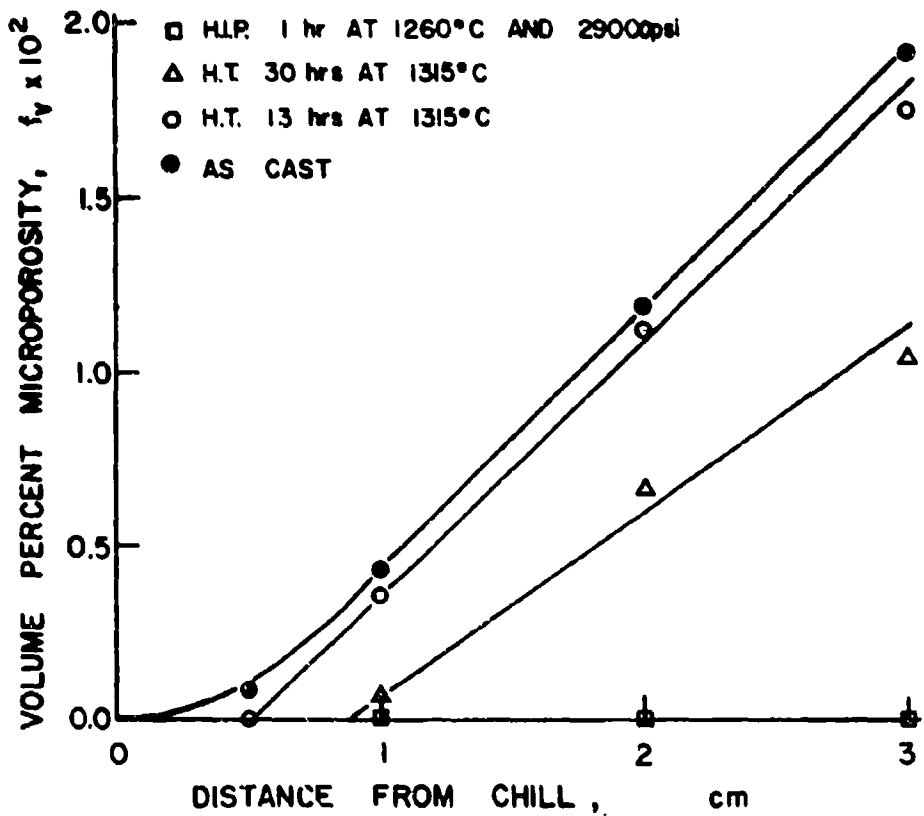


Figure 3. Measured volume percent microporosity versus distance from the chill for the as-cast material, material homogenized for 13 and 30 hours at 1315°C and material hot isostatically pressed for 1 hour at 1960°C and 29,000 psi.

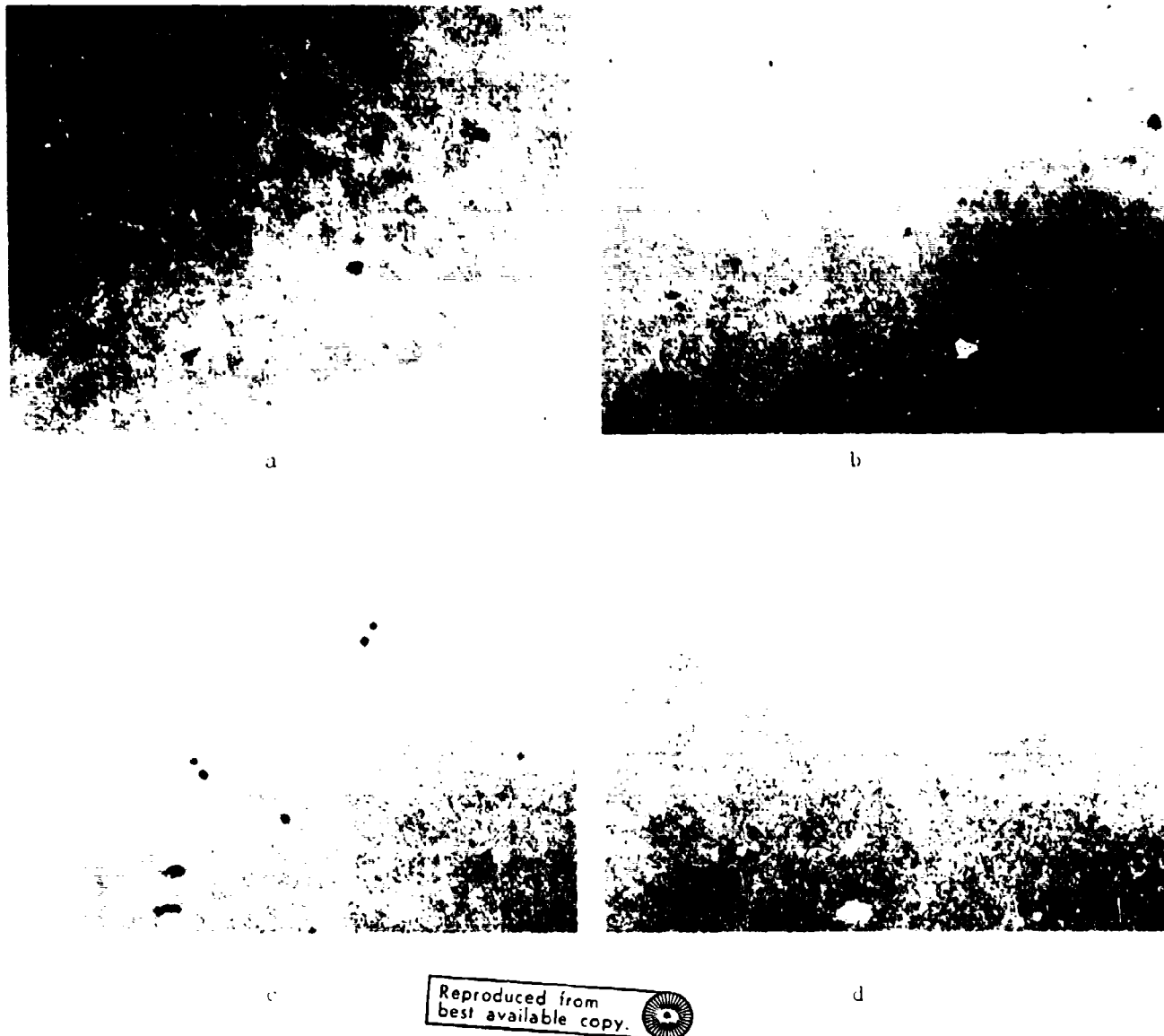


Figure 4. X-ray microradiographs of specimens taken at 3 cm from the chill from Ingot #1, magnification 125X; (a) as-cast material, (b) and (c) material homogenized at 1315°C for 13 and 30 hours, respectively, (d) material hot isostatically pressed for 1 hour at 1260°C and 29,000 psi.

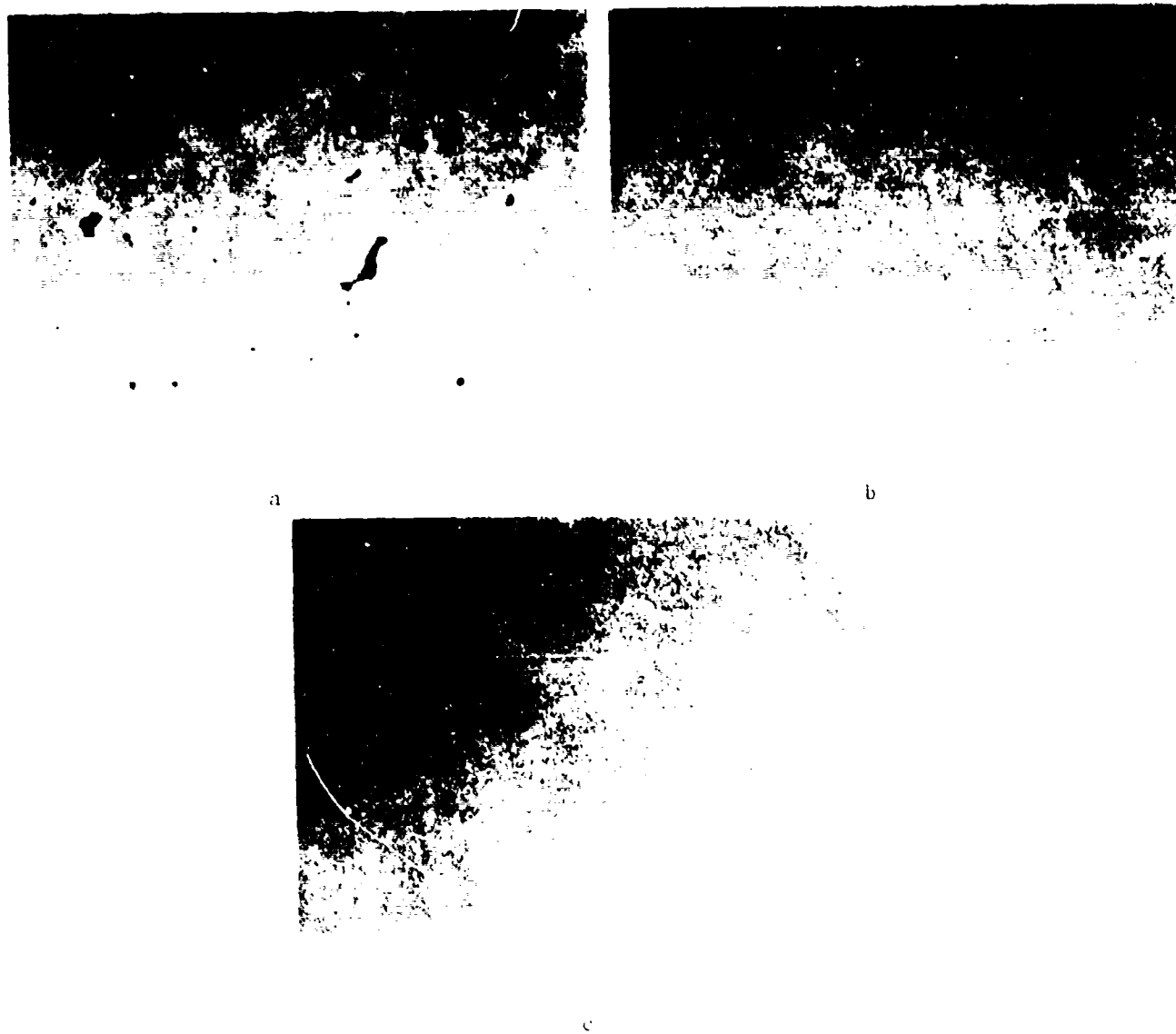


Figure 5. X-ray microradiographs of specimens taken at 3 cm from the chill from Ingot #2, magnification 125X; (a) as-cast material, (b) material hot isostatically pressed for 1 hour at 1260°C and 29,000 psi, (c) material hot isostatically pressed for 1 hour at 1038° and 27,000 psi.

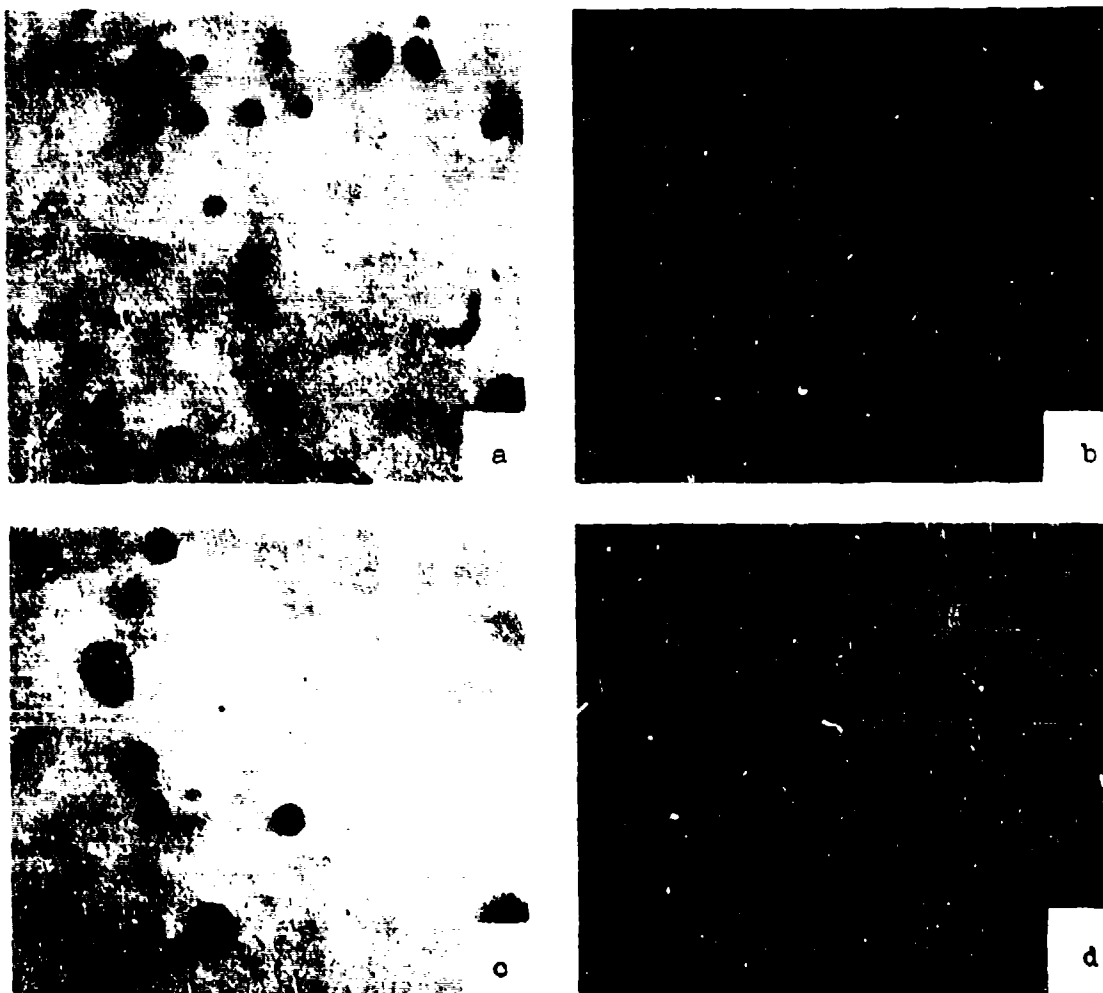


Figure 6. Photomicrographs illustrating the effect of homogenization treatment at 1315°C on Type I sulfides, 1230X. Specimens taken from Ingot H-11 at 2.5 cm from chill. (a) As-cast material, (b), (c), and (d) material homogenized for 10, 20, and 50 hours, respectively.

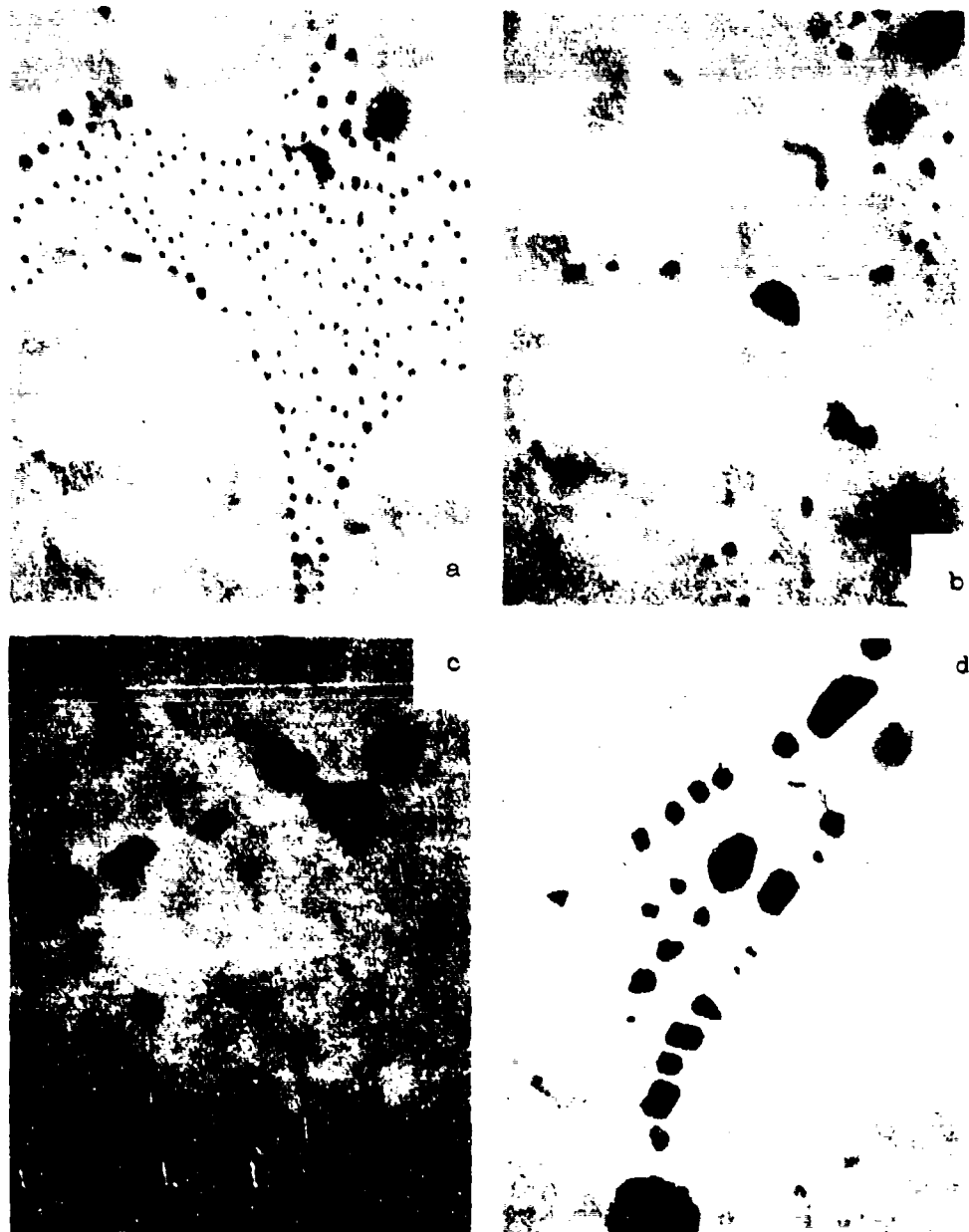


Figure 7. Photomicrographs illustrating the effect of homogenization treatment at 1315°C on Type II sulfides, 1230X. Specimens taken from ingot II-6 at 2.5 cm from chill. (a) As-cast material, (b), (c), (d), and (e) material homogenized for 5, 10, 20, 25 and 30 hours, respectively.



Figure 7.

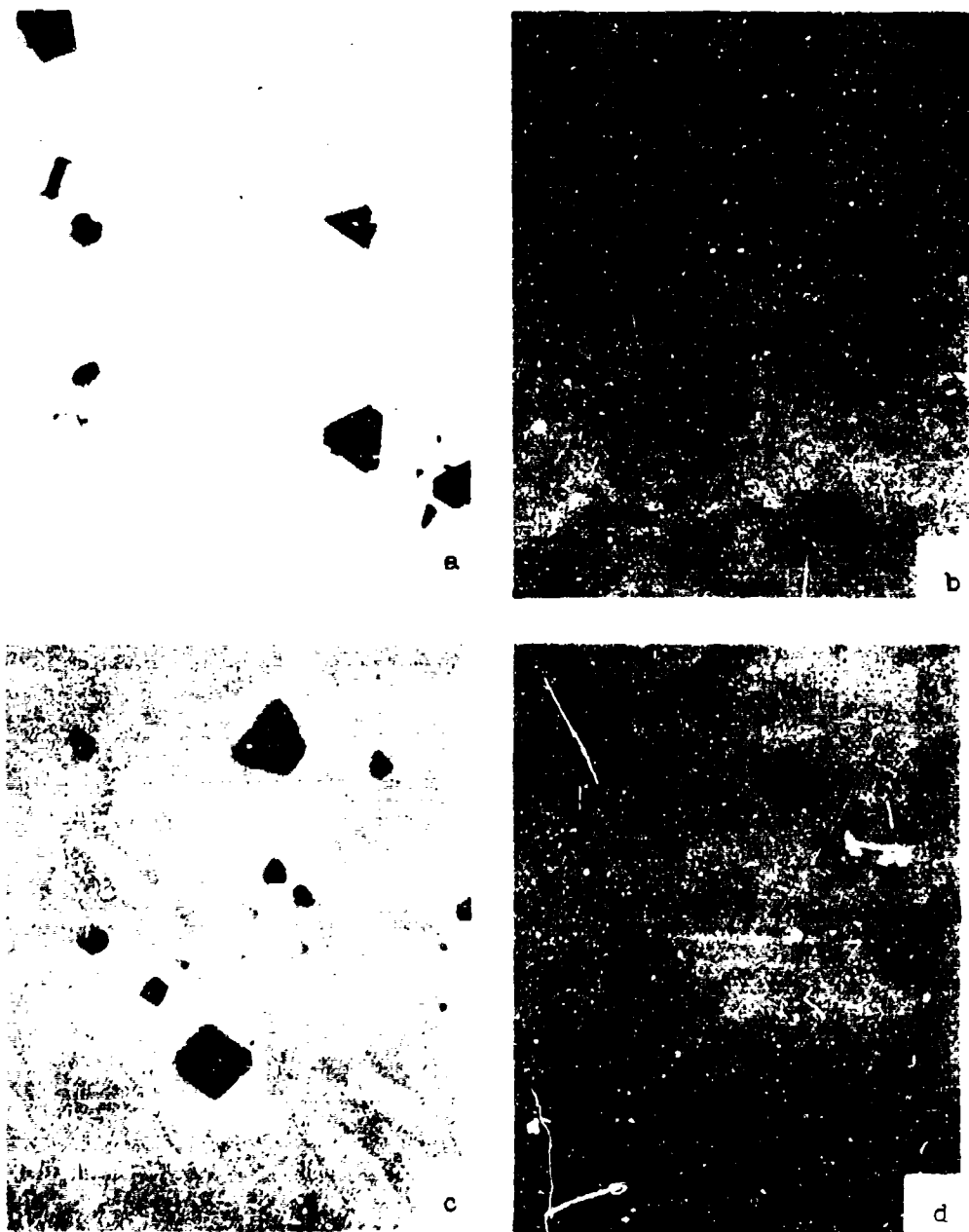


Figure 8. Photomicrographs illustrating the effect of homogenization treatment at 1100°C on Type III sulfides, 615K. Specimens taken from Ingot II-2 at 2.5 cm from chill. (a) As-cast material, (b), (c), and (d) material homogenized for 10, 20 and 50 hours, respectively.

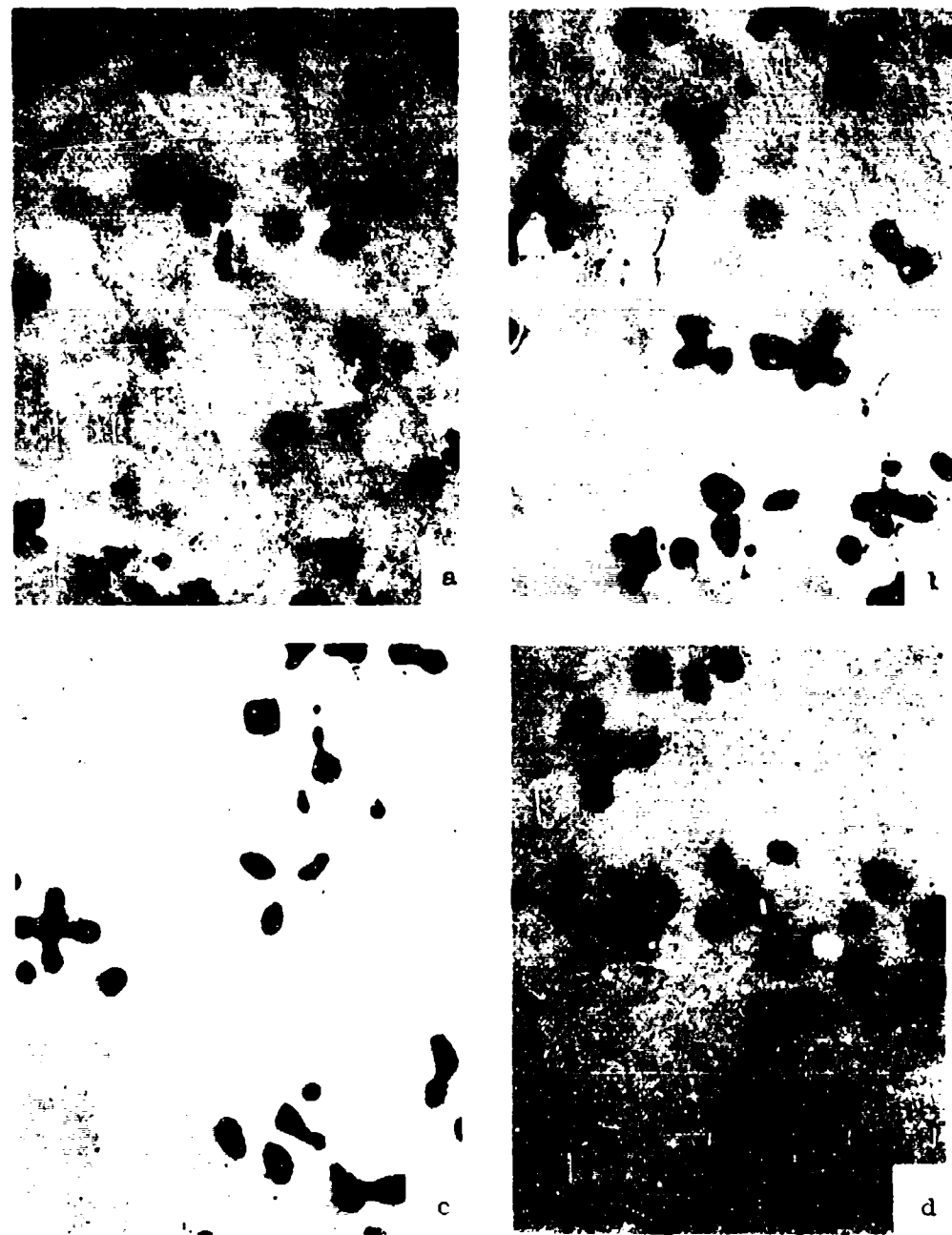


Figure 9. Photomicrographs illustrating the effect of homogenization treatment at 1100°C on Type IV sulfides, 250X. Specimens taken from ingot H-10 at 2.5 cm from chill. (a) As-cast material, (b), (c), (d), and (e) material homogenized for 10.25, 20, 50 and 150 hours, respectively.



Figure 9.

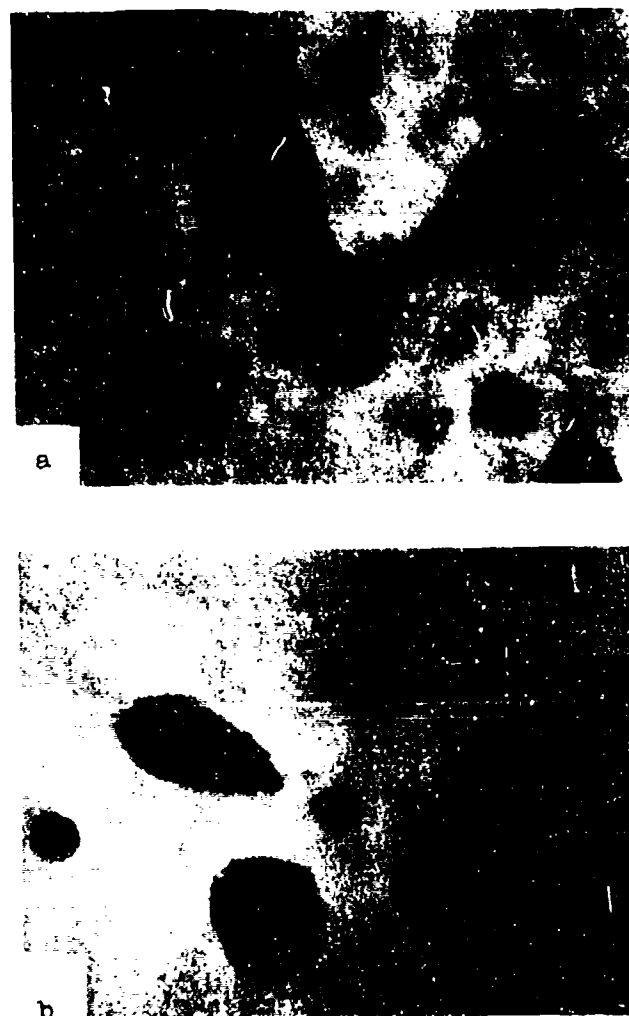


Figure 10. Photomicrographs illustrating coarsening of Type IV sulfides, 1230X. Specimens taken from Ingot If-10 at 0.5 cm from chill.
(a) Homogenized for 10.25 hours and
(b) homogenized for 150 hours.

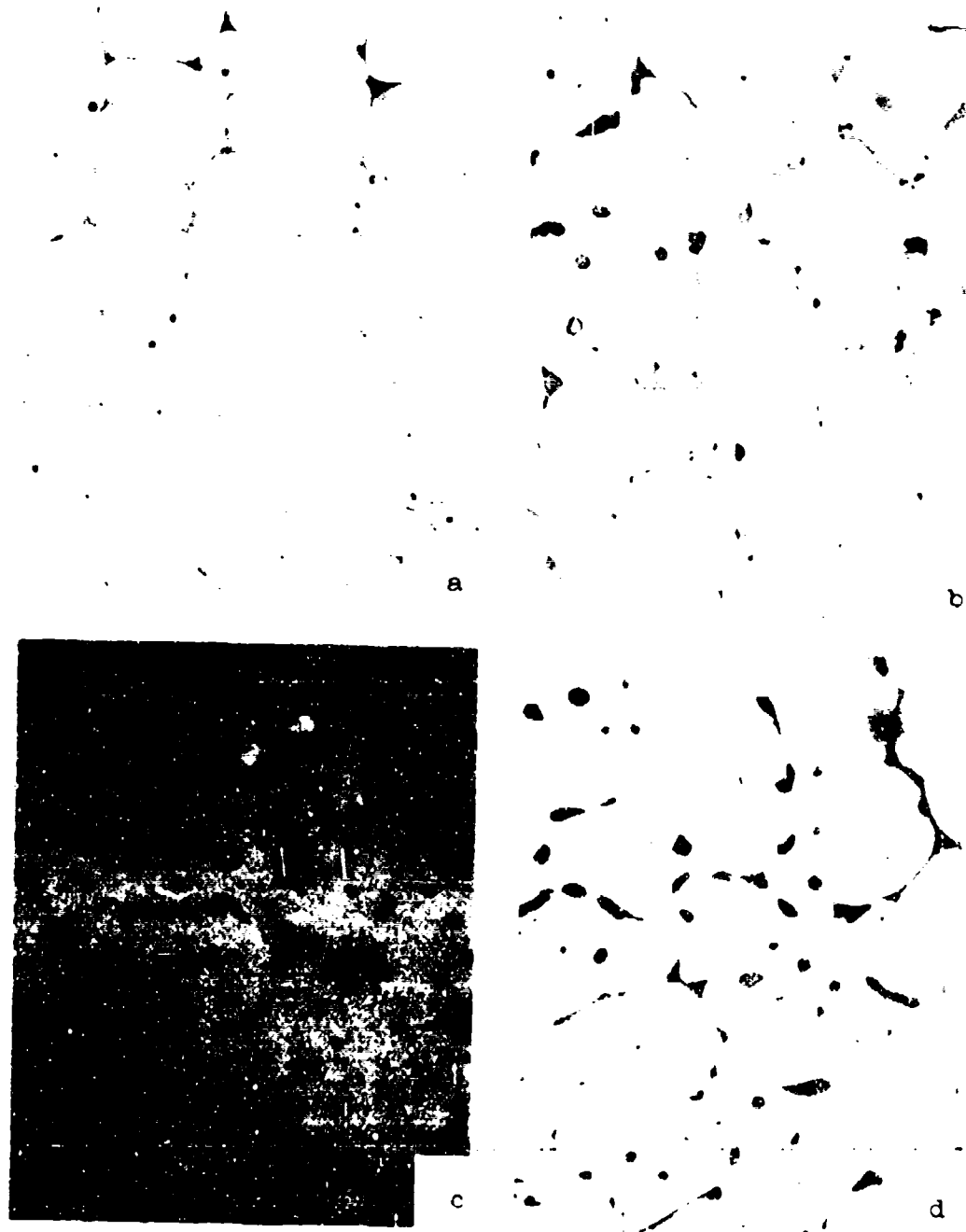


Figure 11. Photomicrographs illustrating the effect of homogenization treatment at 955°C on sheet-like FeS inclusions, 290X. Specimens taken from Ingot II-4 at 2.5 cm from chill.
(a) As-cast material (b), (c) and (d) material homogenized for 20, 40 and 80 hours, respectively.

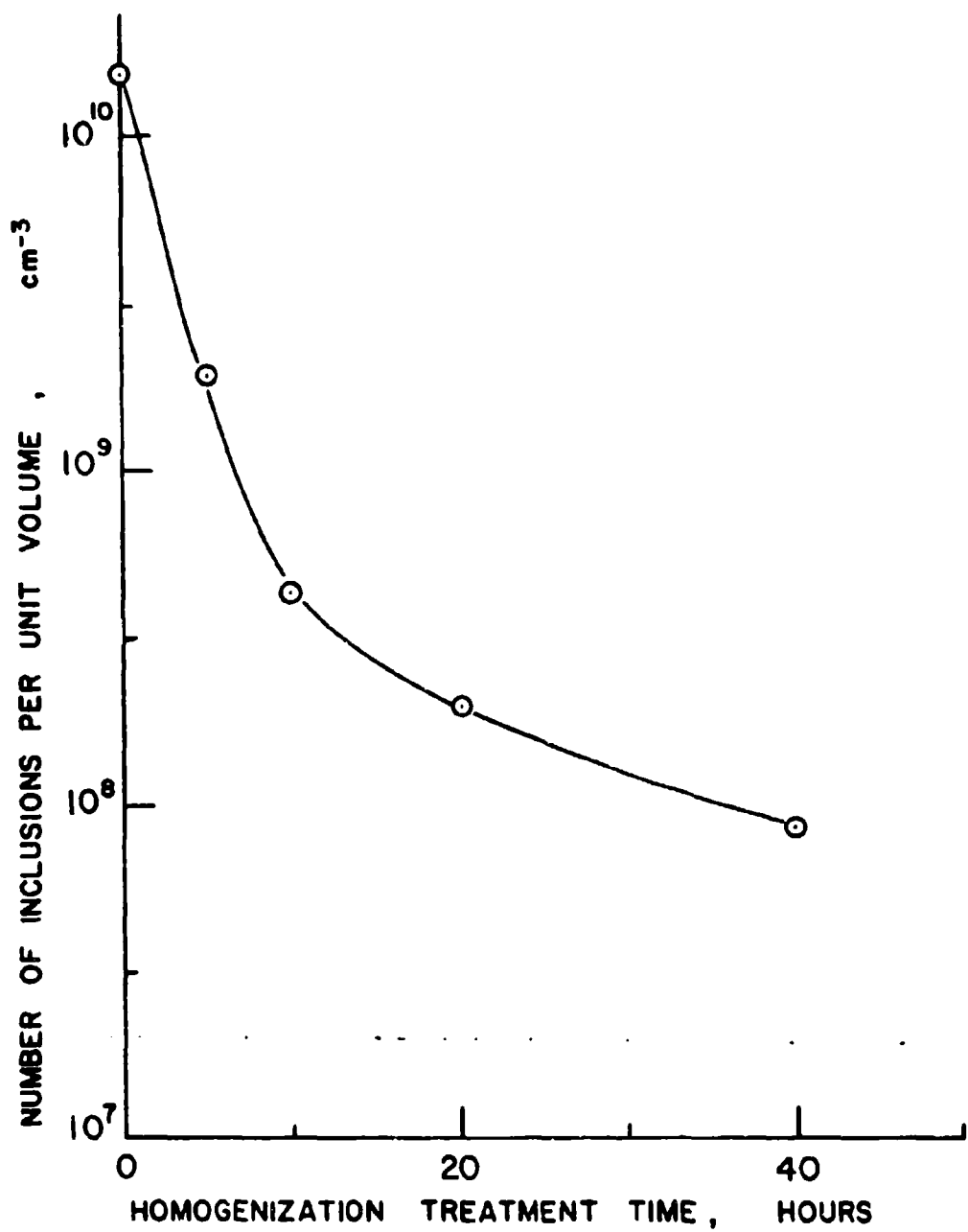


Figure 12. Change of number of sulfide inclusions per unit volume with homogenization treatment time.

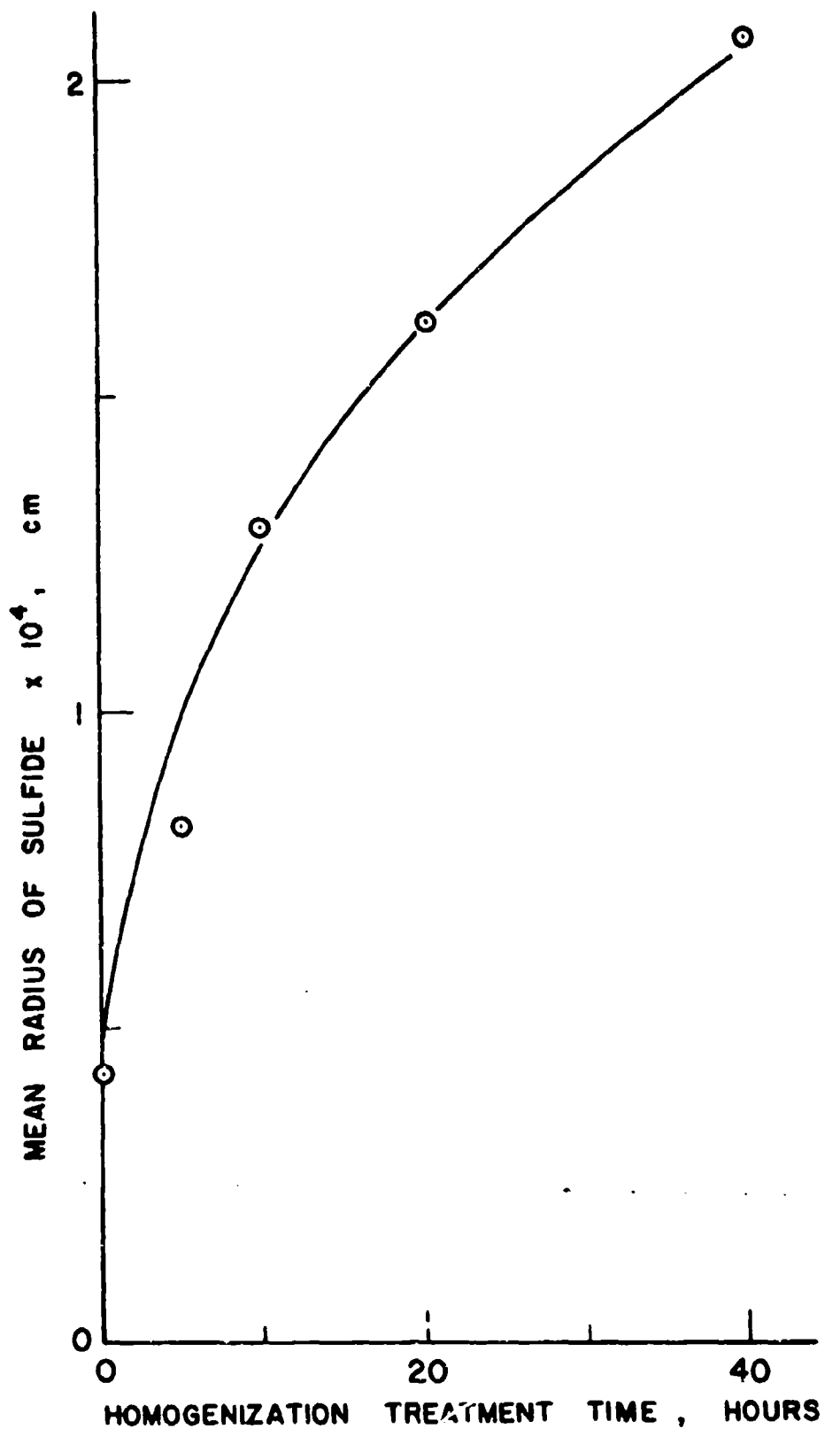


Figure 13. Change of mean radius of sulfides with homogenization treatment time.

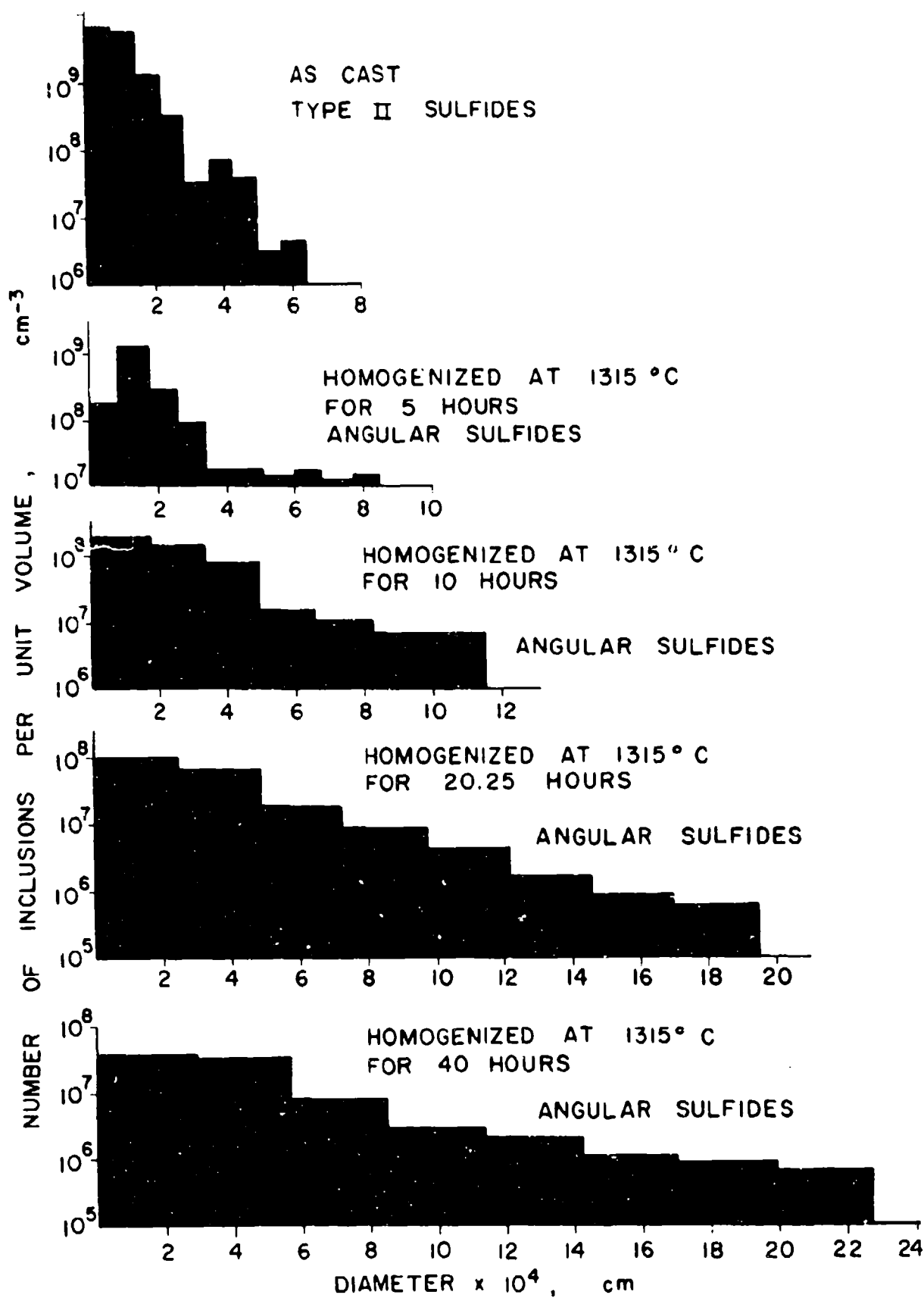


Figure 14. Size distribution of sulfides in the as-cast and homogenized conditions (assuming spherical shape).

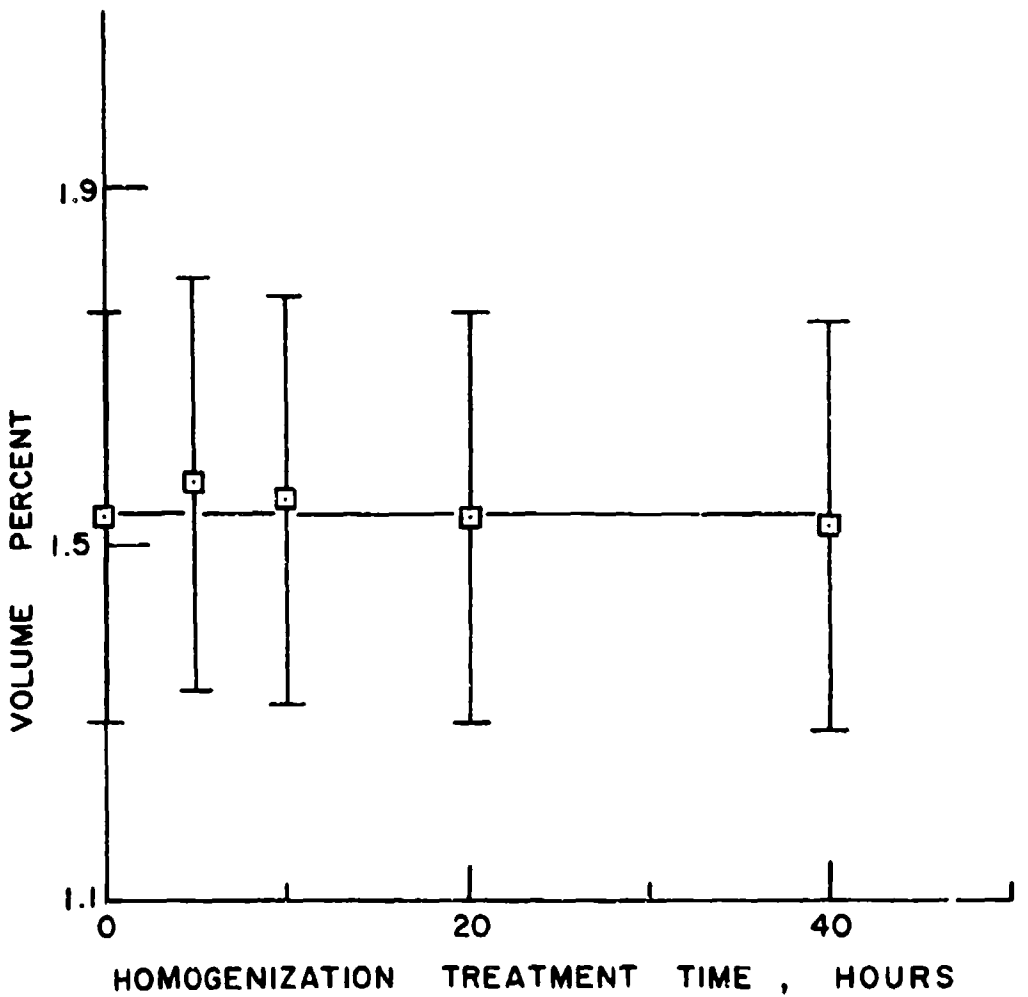


Figure 15. Volume percent sulfides versus homogenization treatment time.

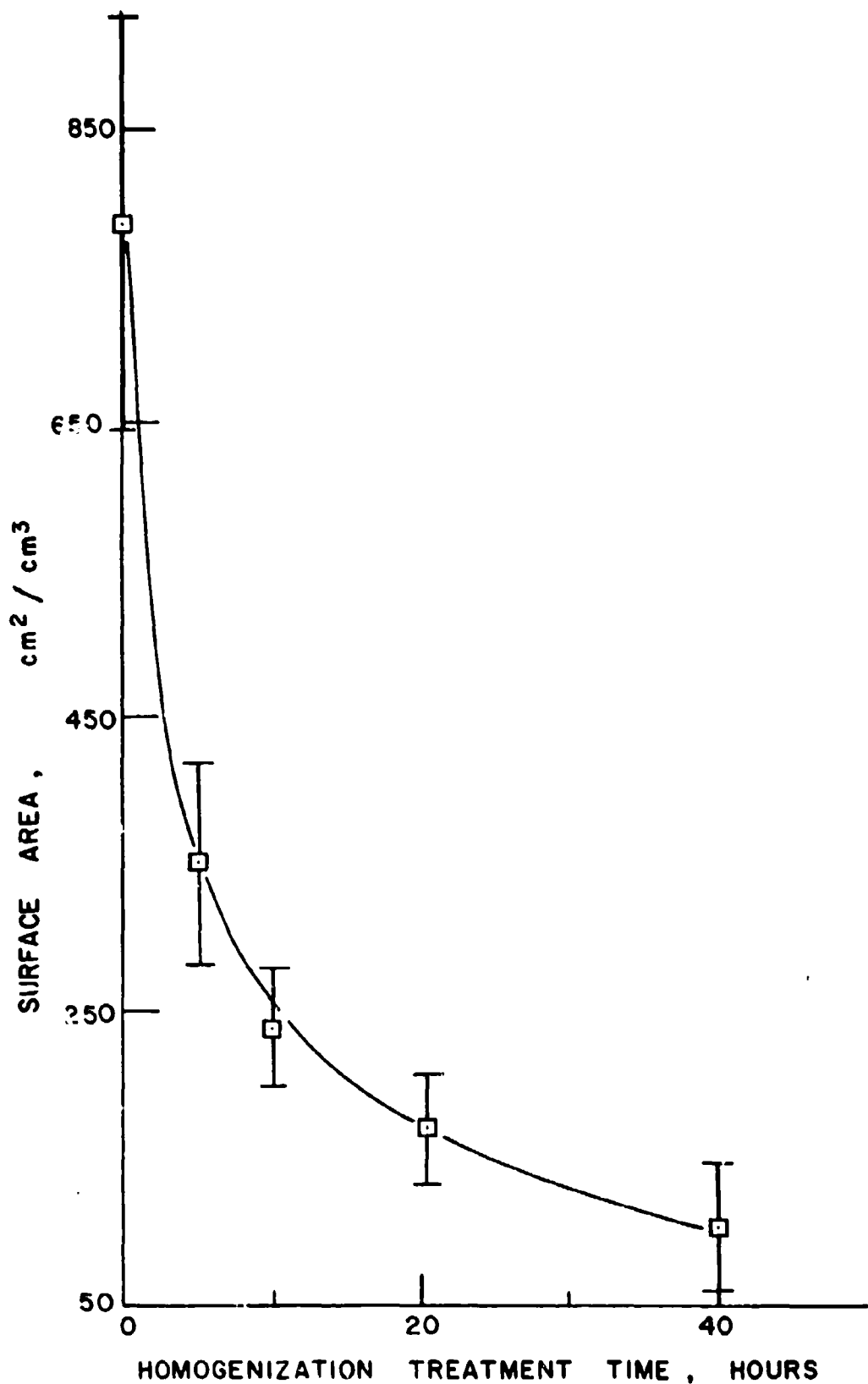


Figure 16. Change of surface area of sulfides per unit volume with homogenization treatment time.

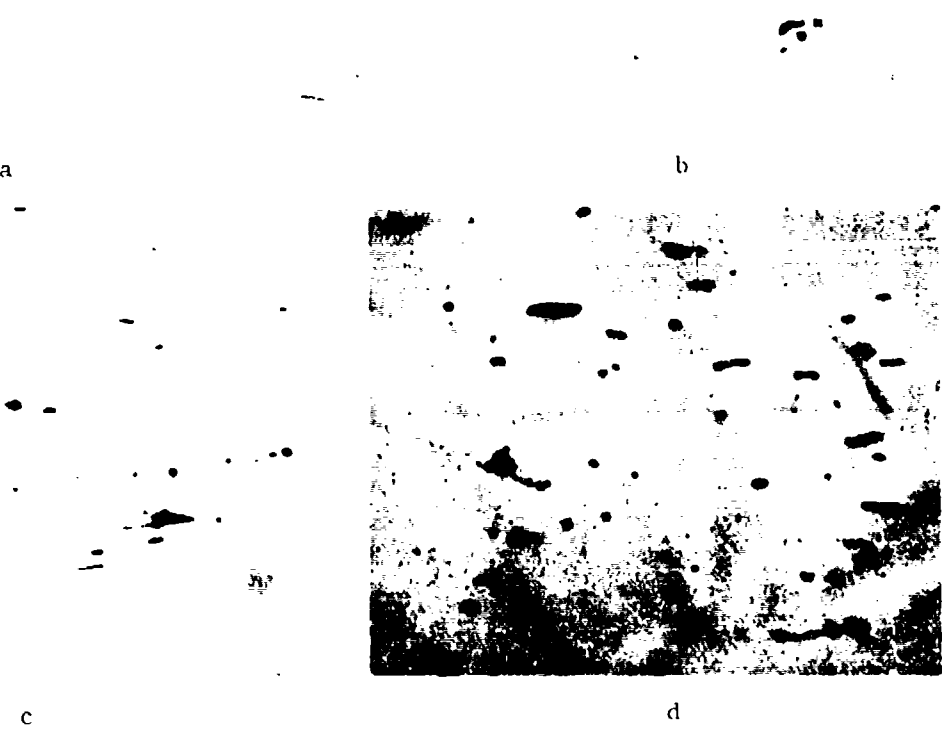


Figure 17. Photomicrographs of cast-and-rolled AISI 4340 unidirectionally solidified low alloy steel, reduction 85%: (a) 0.505 inches from chill, 800X, (b) 2.8 inches from chill, 800X, (c) 4.2 inches from chill, 1000X, (d) 4.2 inches from chill, 1200X.

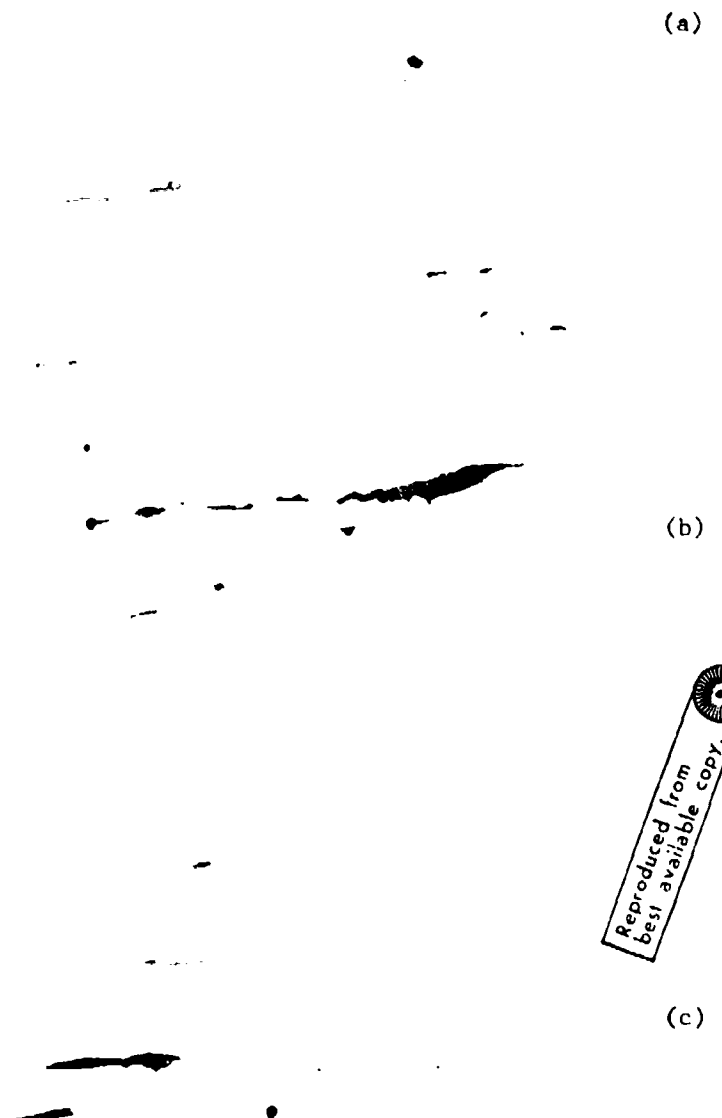


Figure 18. Photomicrographs of cast-and-rolled AISI 4340 unidirectionally solidified low alloy steel. Reduction 70%. 800X. (a) 1.54 inches from chill, (b) and (c) 2.8 inches from chill.

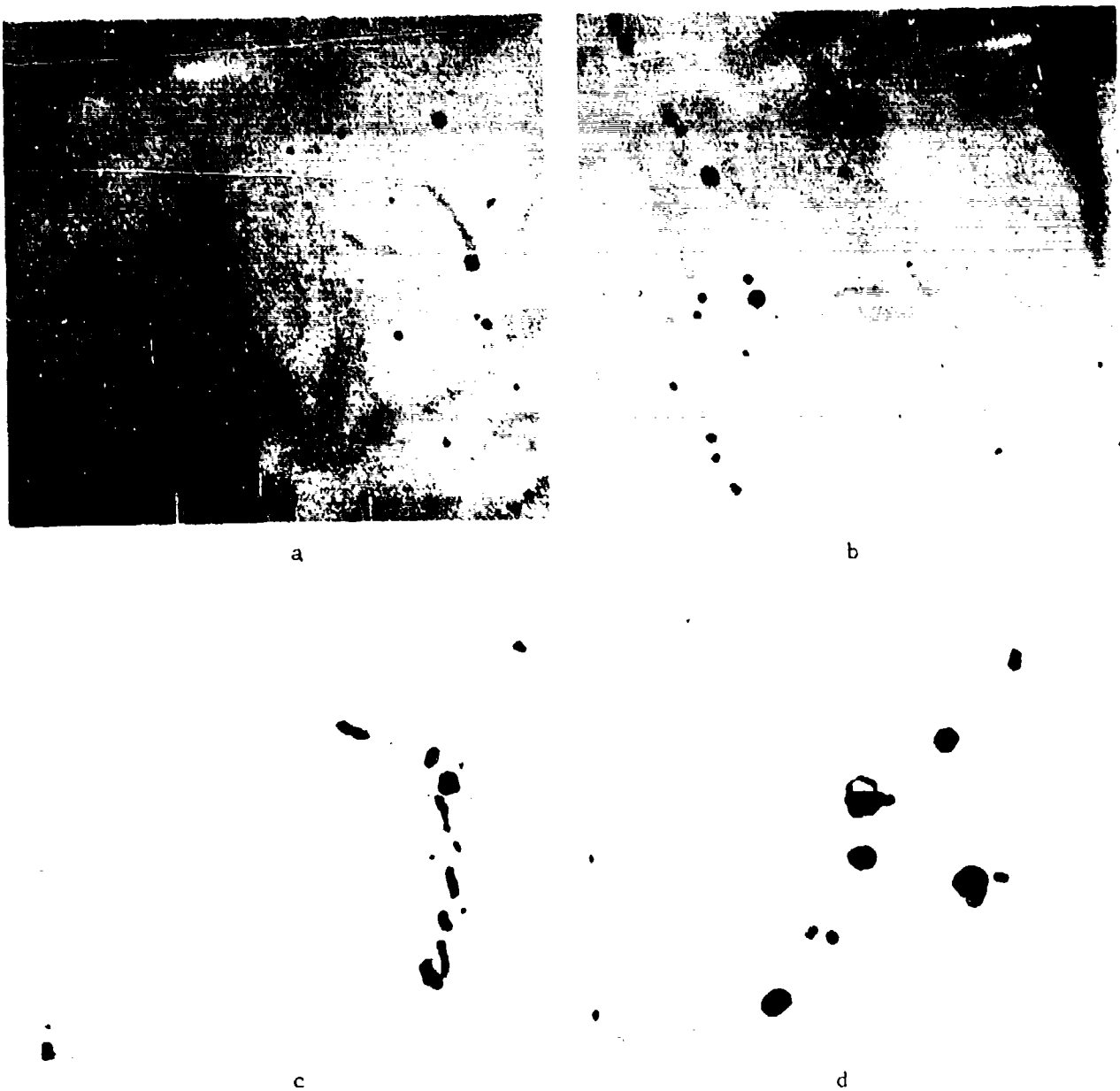


Figure 19. Photomicrographs of cast-and-rolled AISI 4340 directionally solidified low alloy steel. Reduction 85%, 800X. Specimens taken at 1.54 inches from chill and homogenized at 1315°C for: (a) 20 hrs., (b) and (c) 50 hrs., and (d) 100 hrs.



Reproduced from
best available copy.

Figure 20. Photomicrographs of cast-and-rolled AISI 4340 directionally solidified low alloy steel. Reduction 70%, 800X. Specimen taken at 2.8 inches from chill and homogenized at 1315°C for: (a) 50 hrs., (b), (c) and (d) 100 hrs.

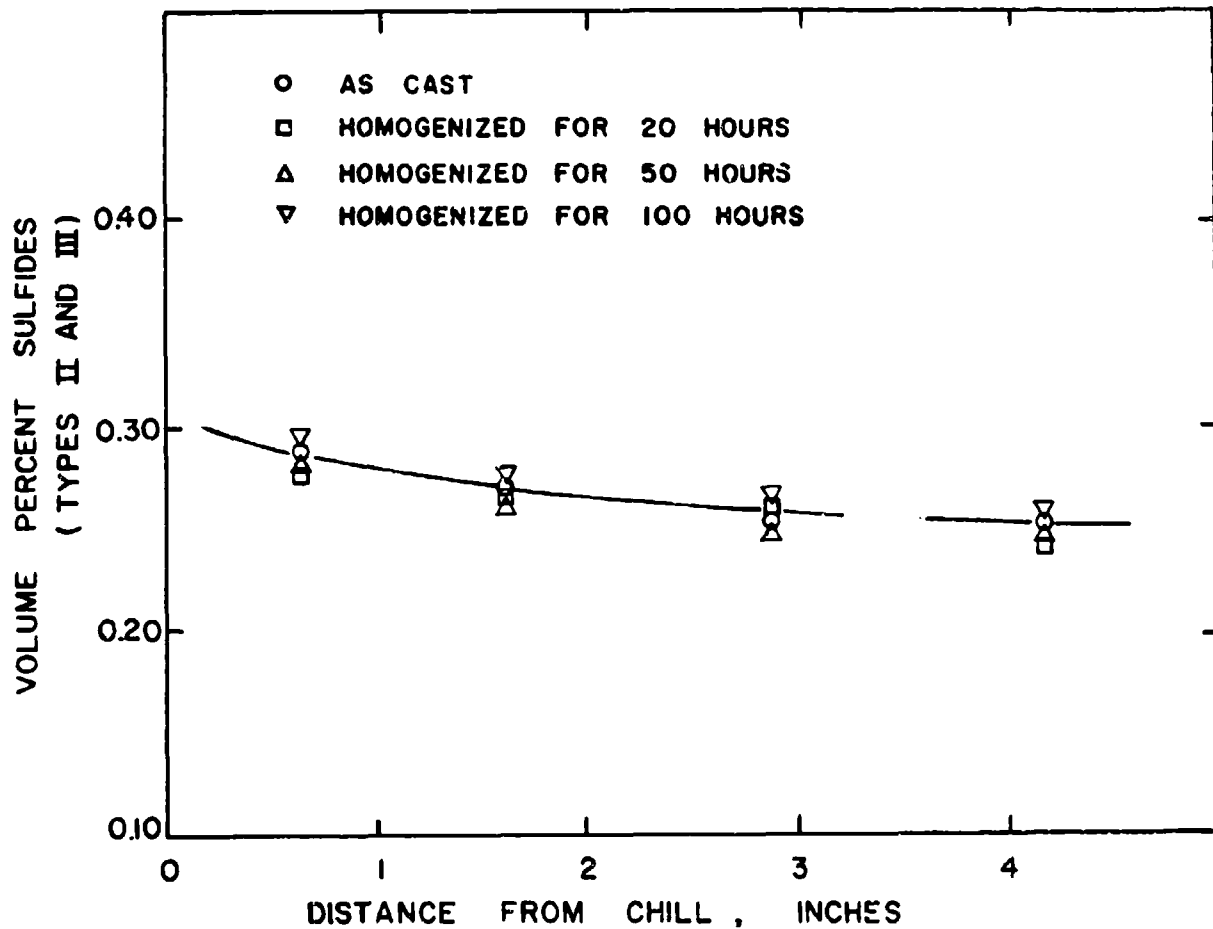


Figure 21. Volume percent sulfides, Types II and III, versus distance from the chill. AISI 4340 unidirectionally solidified low alloy steel. As-cast and cast-and-homogenized specimens at 1315°C for 20, 50 and 100 hours.

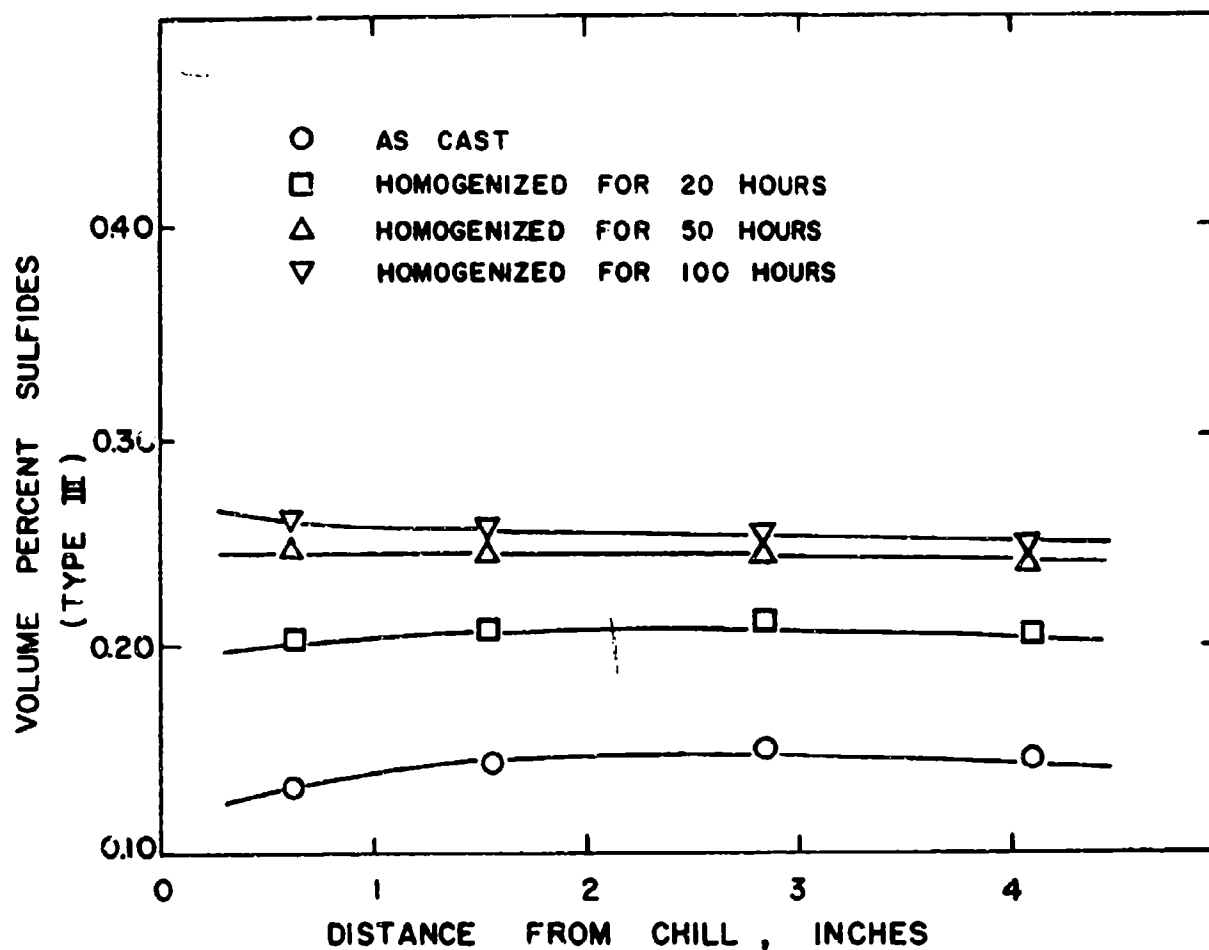


Figure 22. Volume percent sulfides, Type III, versus distance from the chill. AISI 4340 unidirectionally solidified low alloy steel. As-cast and cast-and-homogenized specimen at 1315°C for 20, 50 and 100 hours.

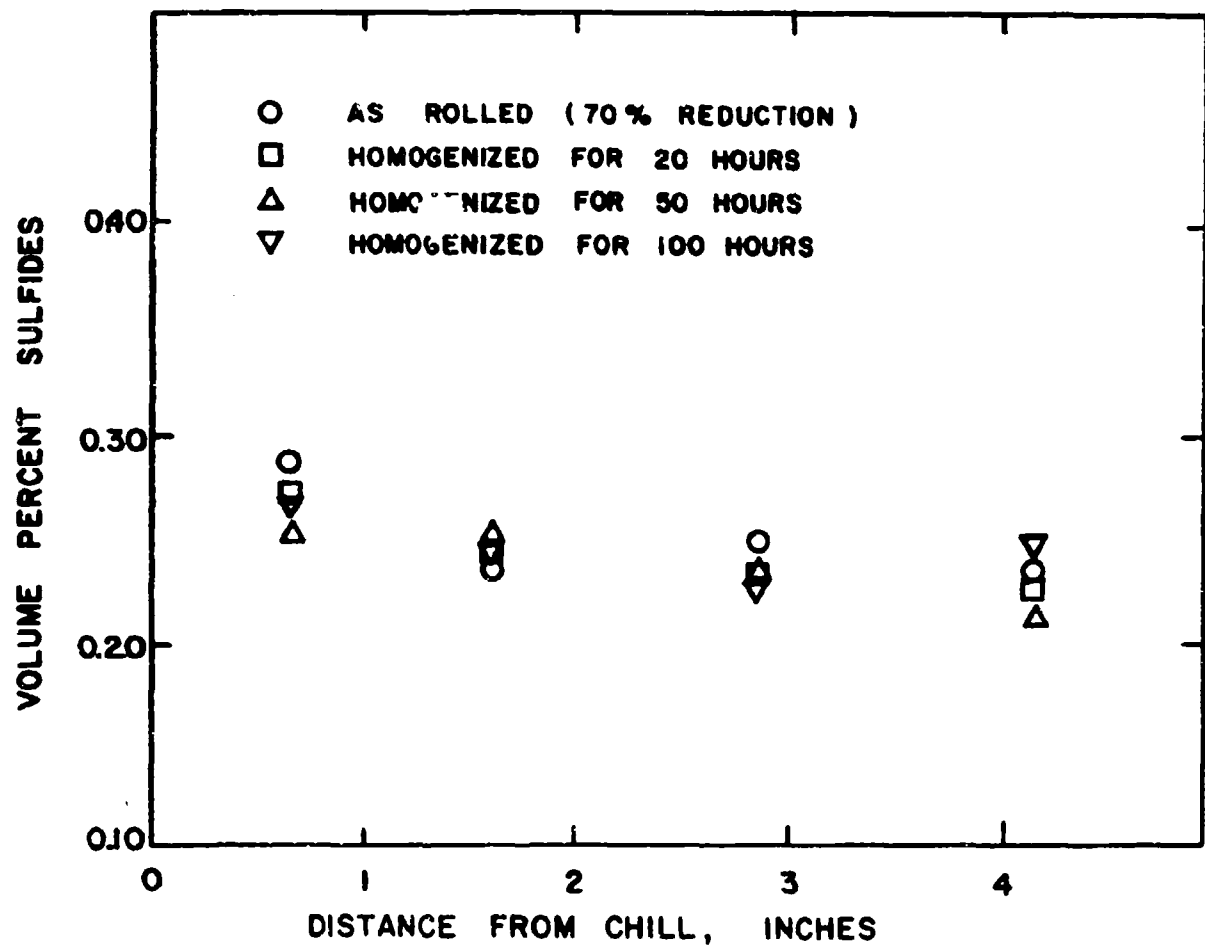


Figure 23. Volume percent sulfides versus distance from the chill.
AISI 4340 unidirectionally solidified low alloy steel.
As-rolled (70% reduction) and rolled-and-homogenized
specimens at 1315°C for 20, 50 and 100 hours.

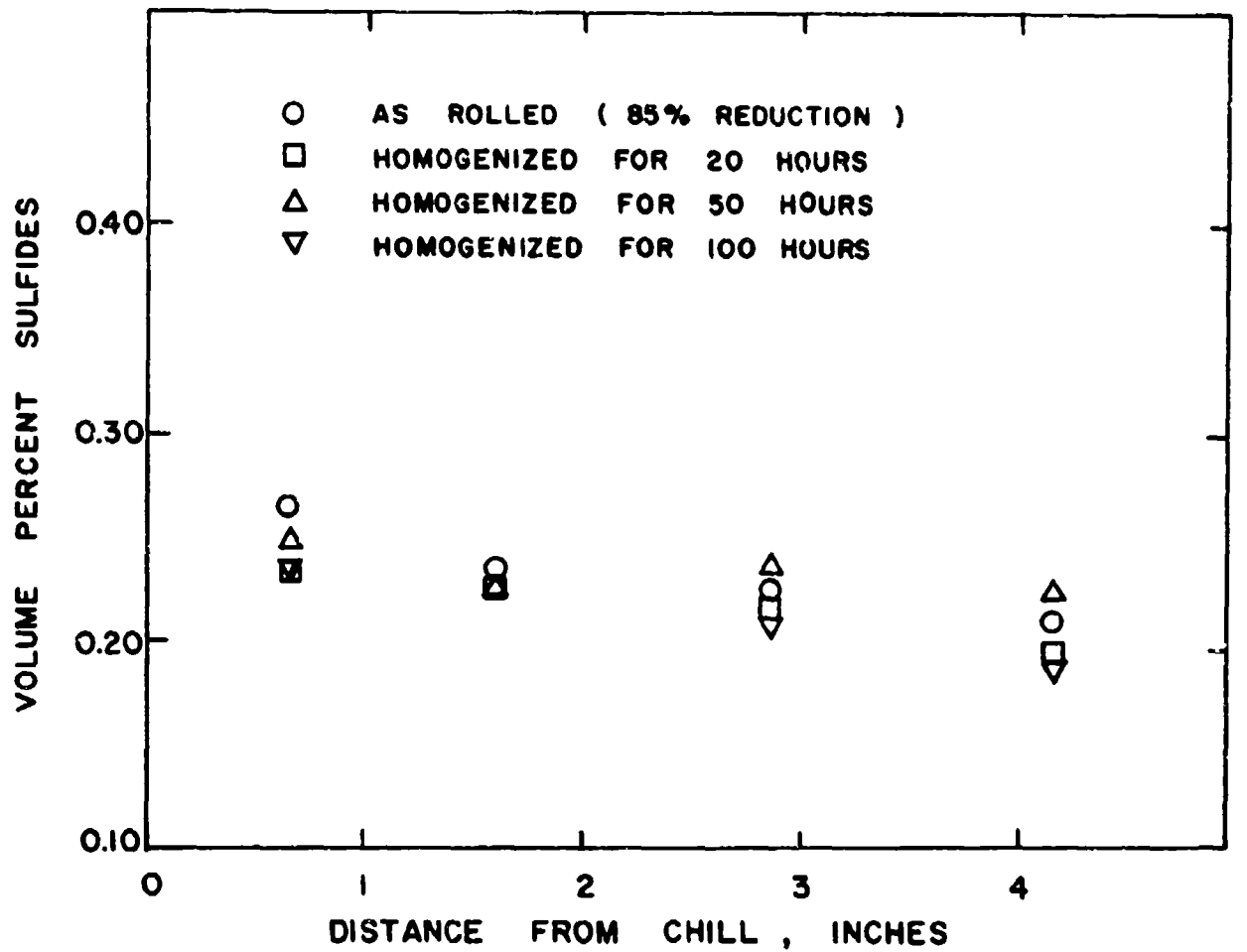


Figure 24. Volume percent sulfides versus distance from the chill. AISI 4340 unidirectionally solidified low alloy steel. As-rolled (85% reduction) and rolled-and-homogenized specimens at 1315°C for 20, 50 and 100 hours.

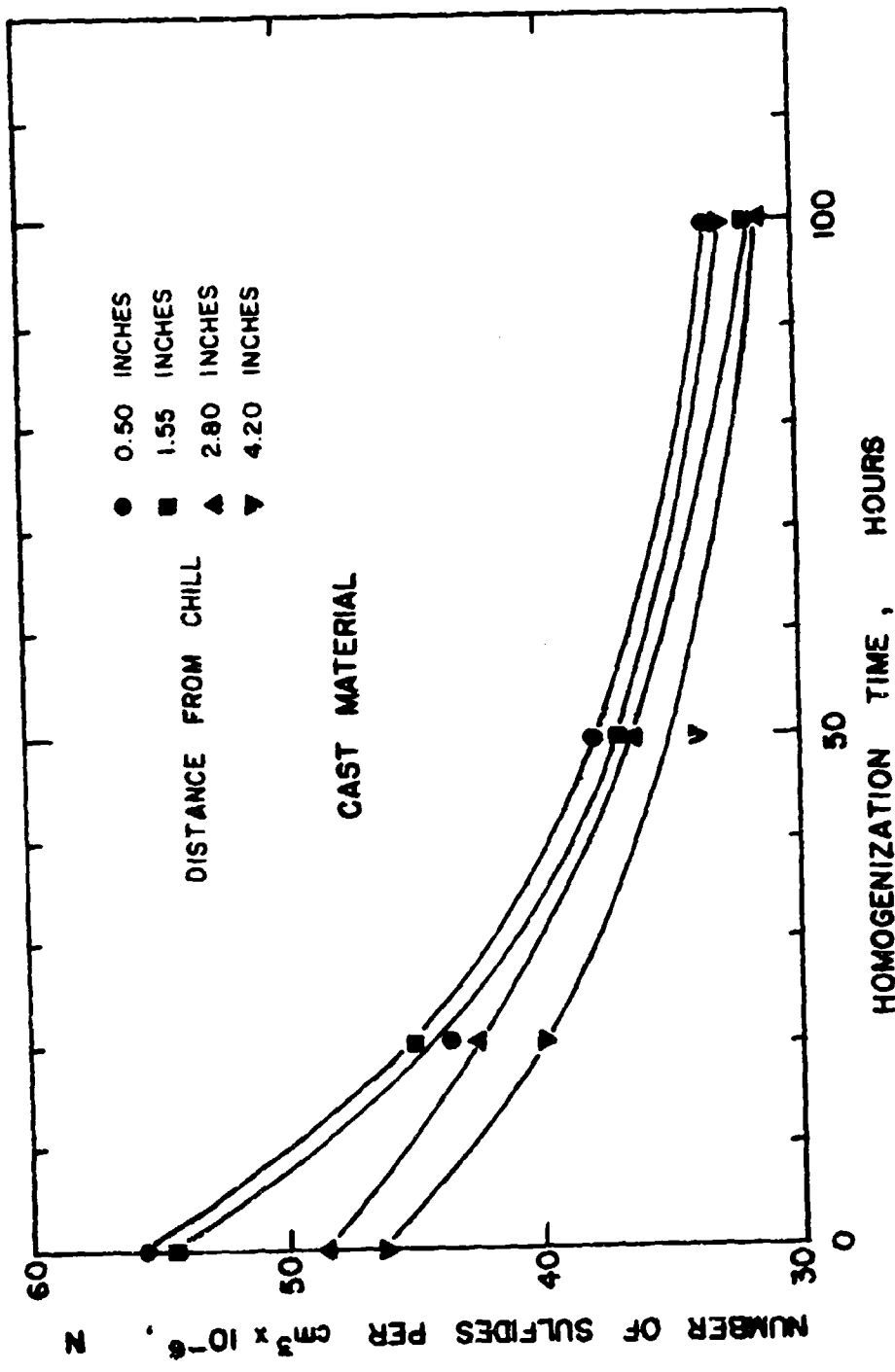


Figure 25. Number of sulfides per unit volume of matrix versus homogenization time. AISI 4340 unidirectionally solidified low alloy steel. Cast material. Specimens taken at different distances from the chill.

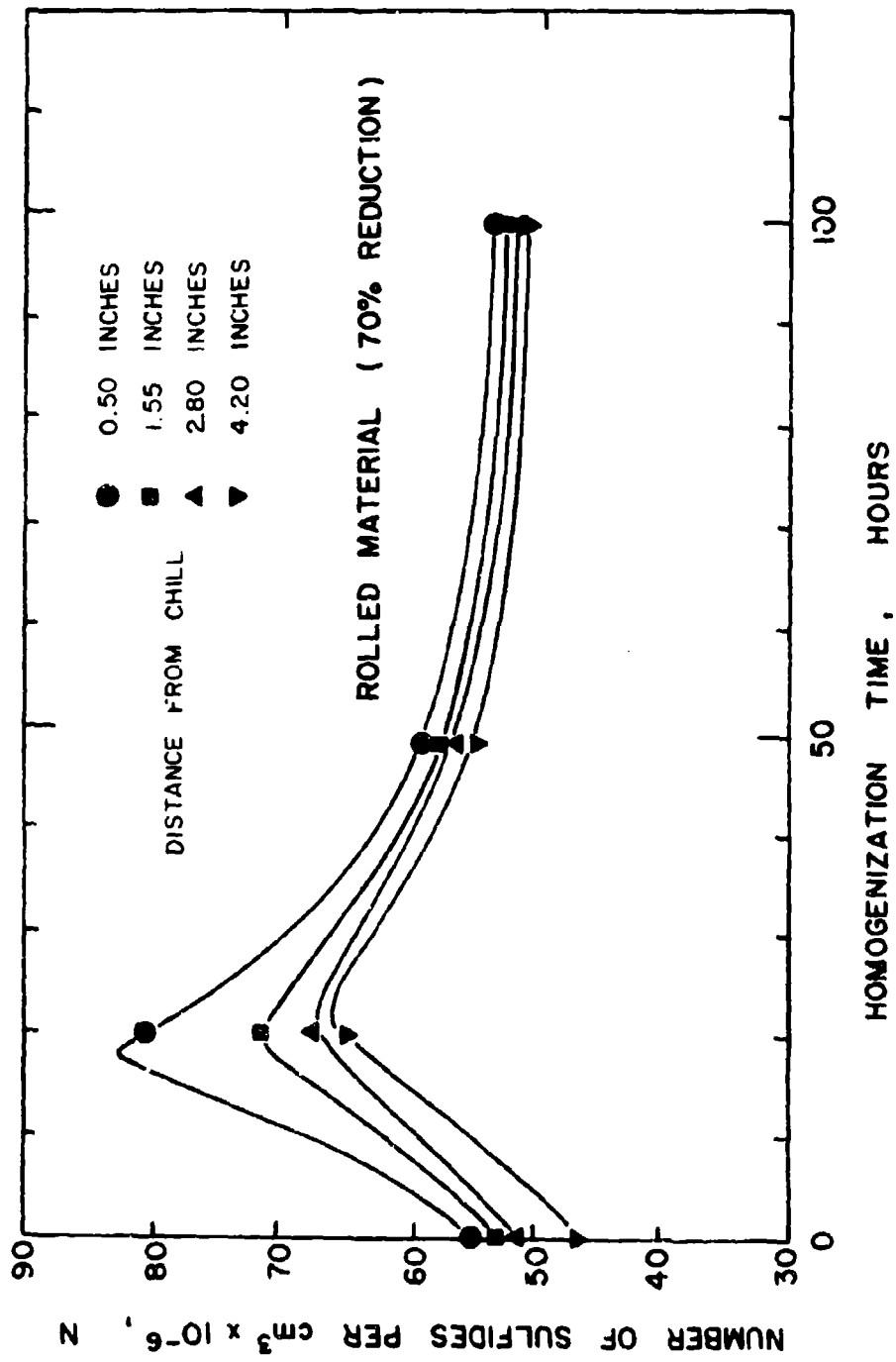


Figure 26. Number of sulfides per unit volume of matrix versus homogenization time. AISI 4340 unidirectionally solidified low alloy steel. Rolled material, reduced 70%. Specimens taken at different distances from the chill.

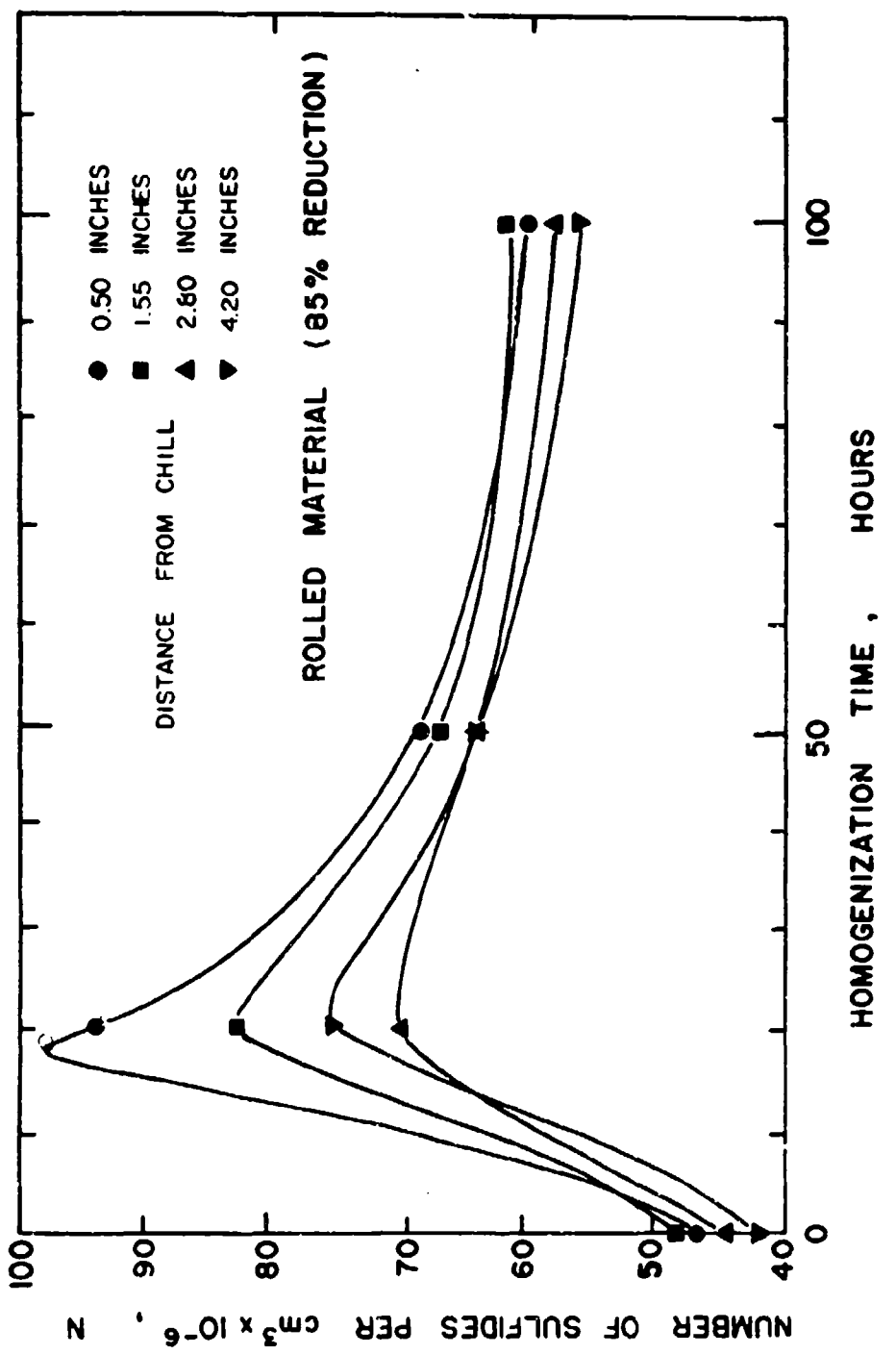


Figure 27. Number of sulfides per unit volume of matrix versus homogenization time. AISI 4340 unidirectionally solidified low alloy steel. Rolled material, reduced 85%. Specimens taken at different distances from the chill.

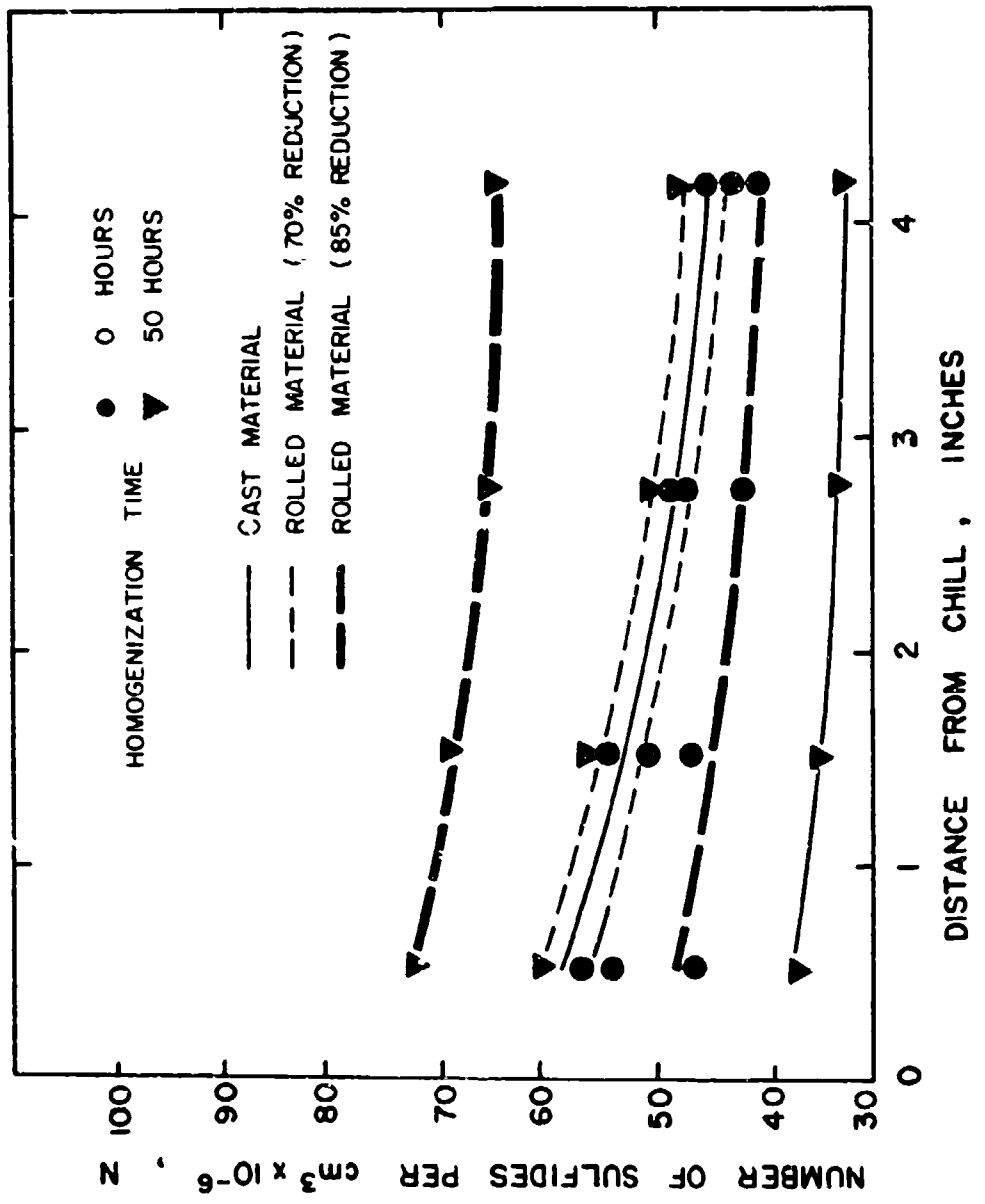


Figure 28. Number of sulfides per unit volume of matrix versus distance from the chill. AISI 4340 unidirectionally solidified low alloy steel. Cast material and rolled material reduced 70% and 85%. Specimens with as-processed condition or homogenized for 50 hours.

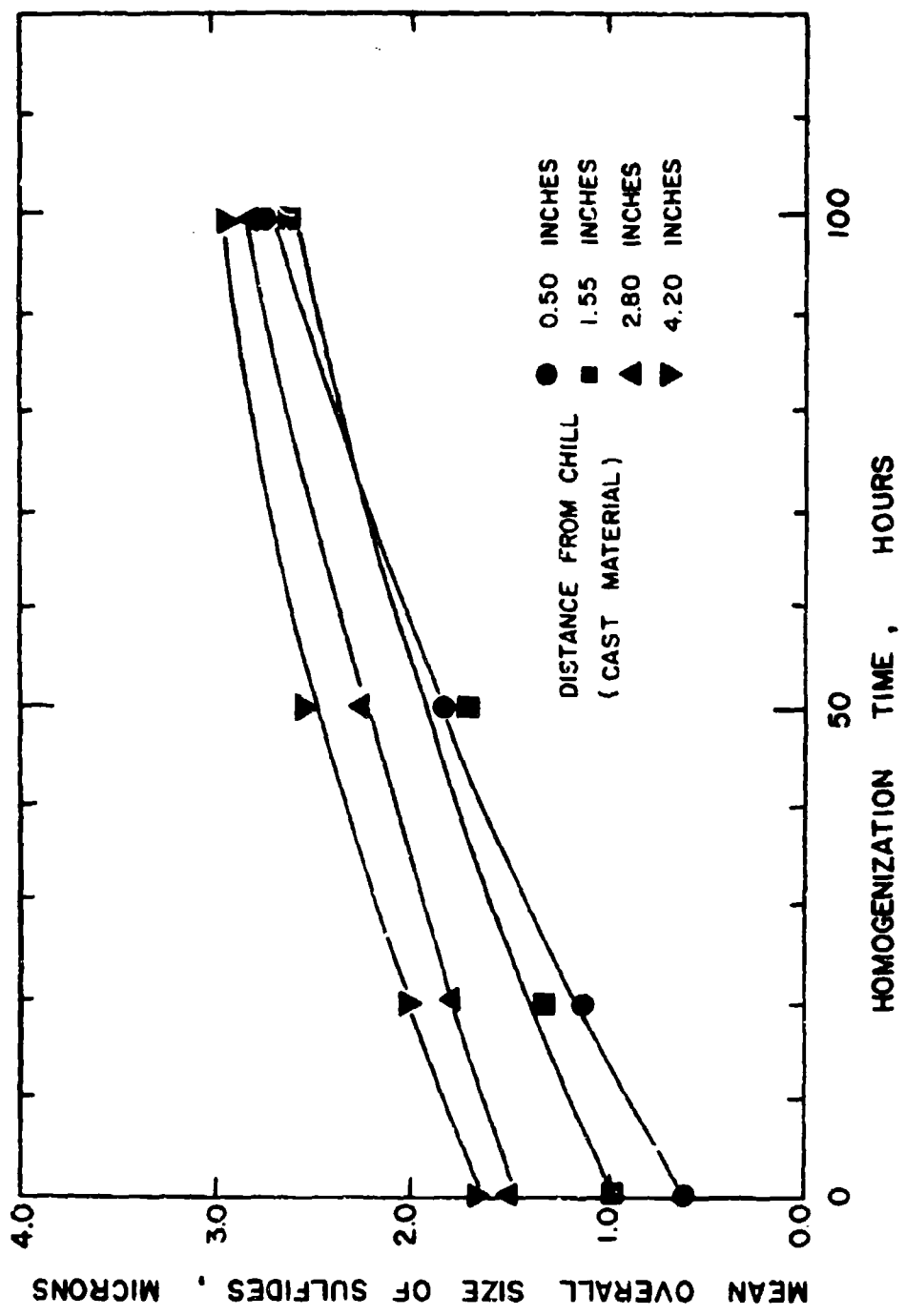


Figure 29. Mean overall size of sulfides versus homogenization time. AISI 4340 unidirectionally solidified low alloy steel. Cast material. Specimens taken at different distances from the chill.

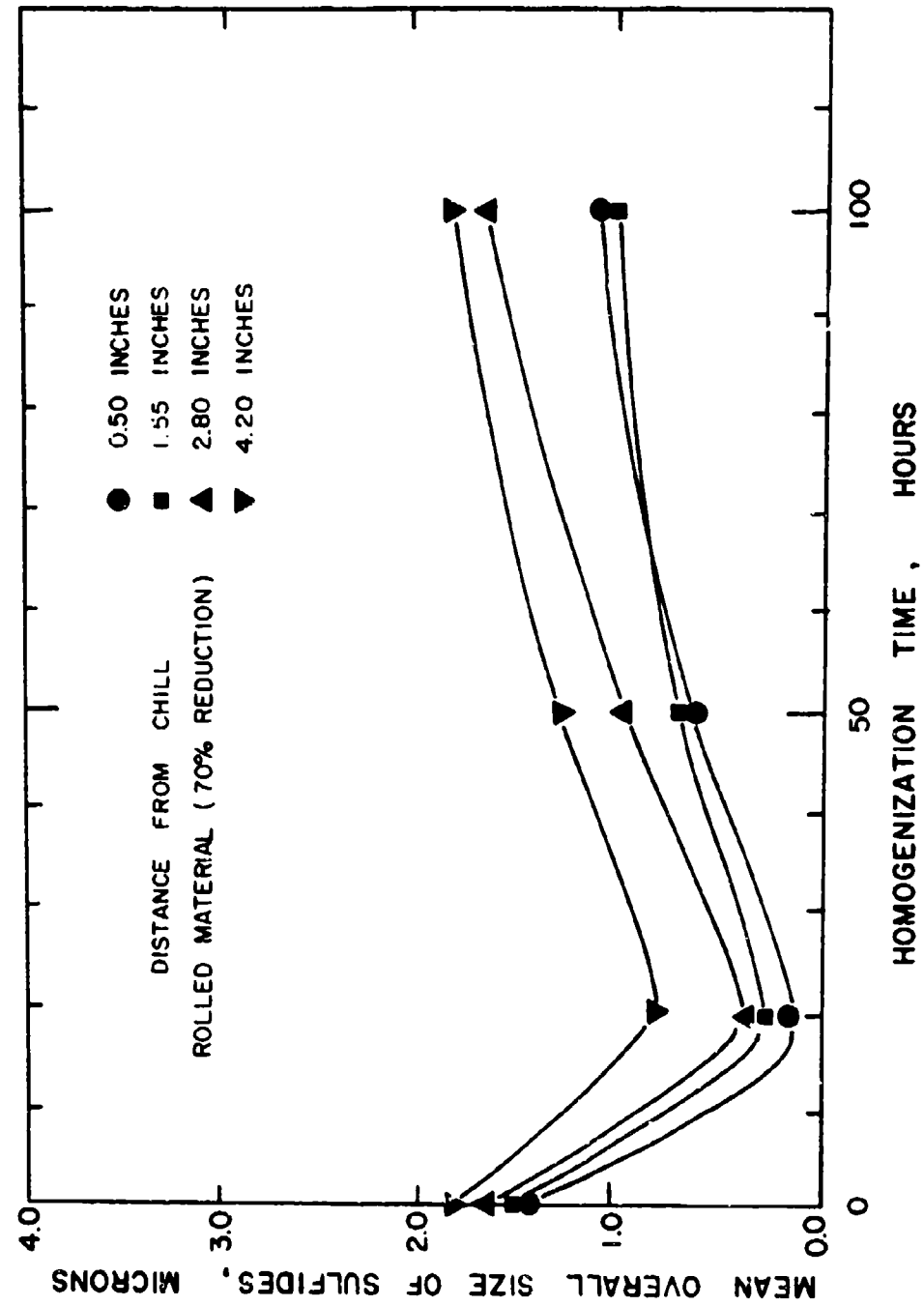


Figure 30. Mean overall size of sulfides versus homogenization time. AISI 4340 unidirectionally solidified low alloy steel. Rolled material reduced 70%. Specimens taken at different distances from the chill.

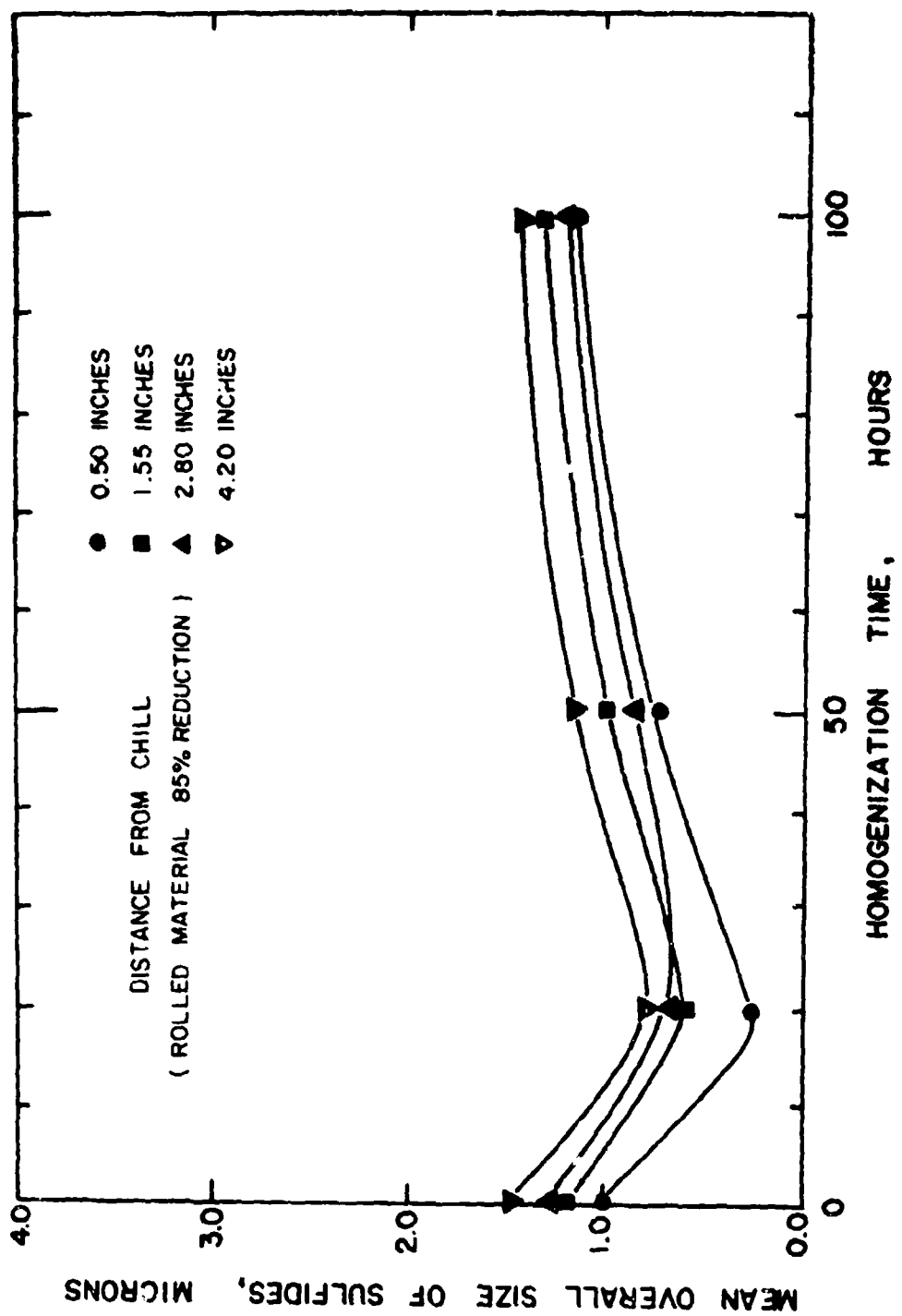


Figure 31. Mean overall size of sulfides versus homogenization time. AISI 4340 unidirectionally solidified low alloy steel. Rolled material reduced 85%. Specimens taken at different distances from the chill.

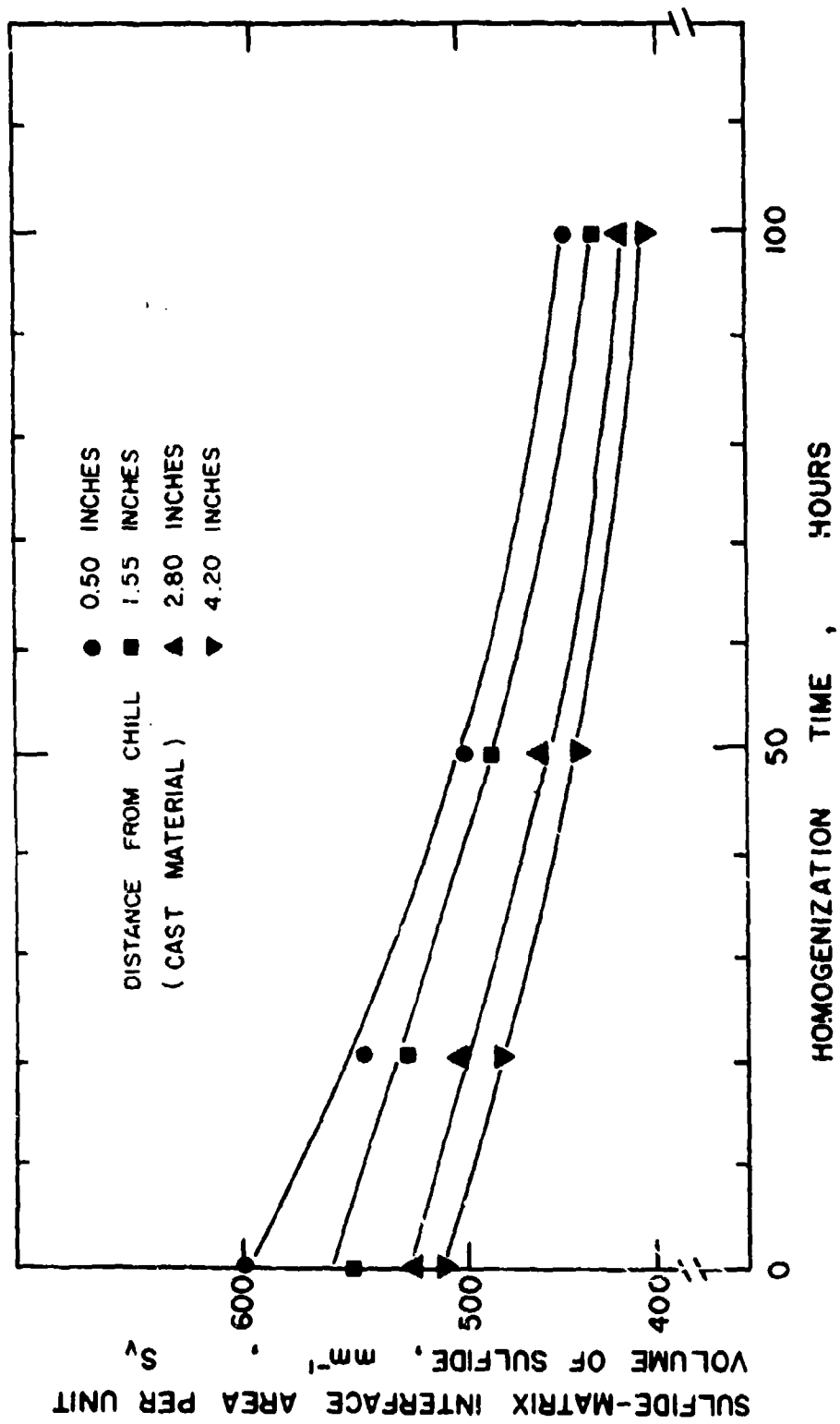


Figure 32. Sulfide-matrix interface area per unit volume of sulfide, S_v , versus homogenization time. AISI 4340 unidirectionally solidified low alloy steel. Cast material. Specimens taken at different distances from the chill.

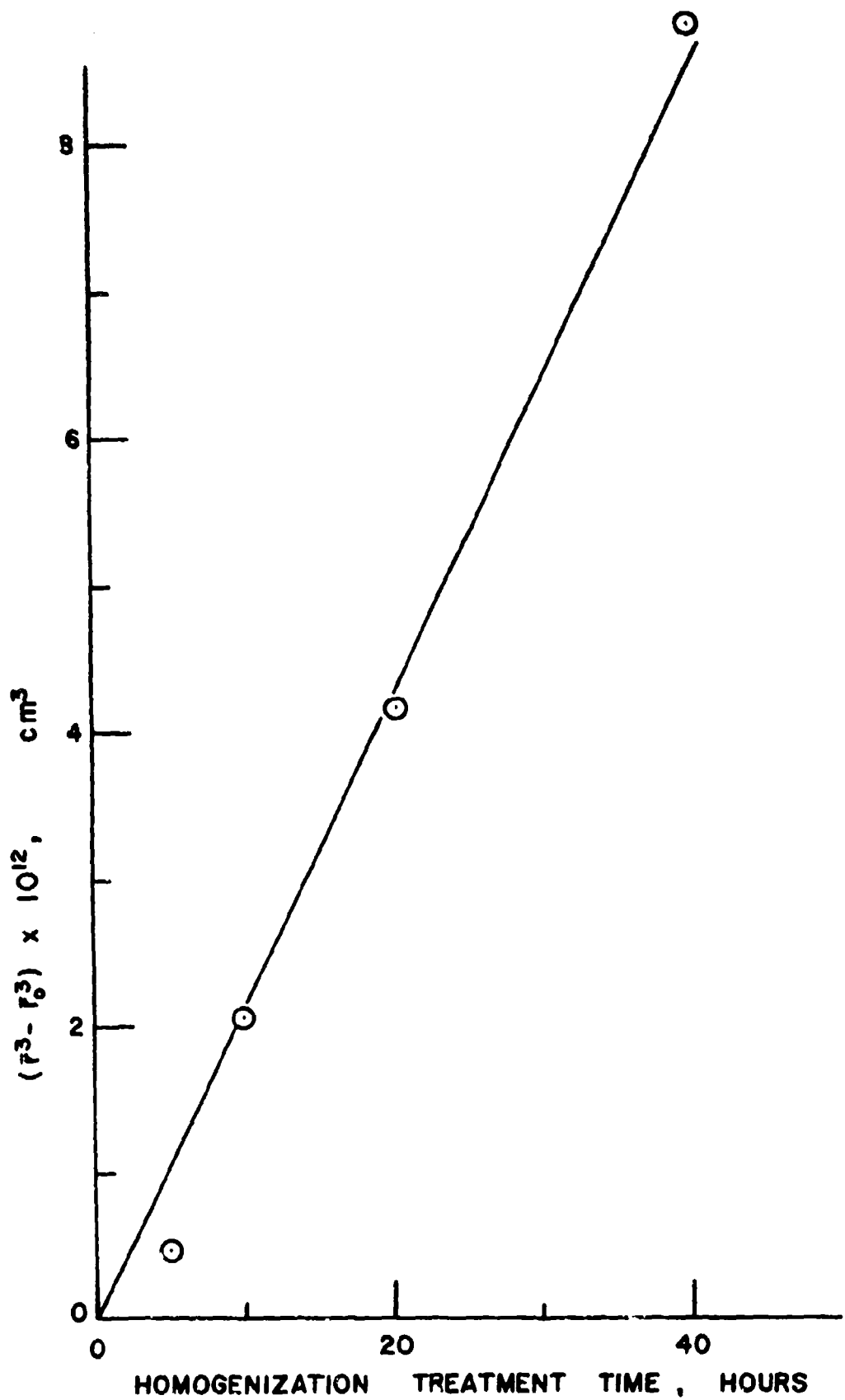


Figure 33. $(\bar{r}^3 - \bar{r}_0^3)$ for sulfides versus homogenization treatment time.

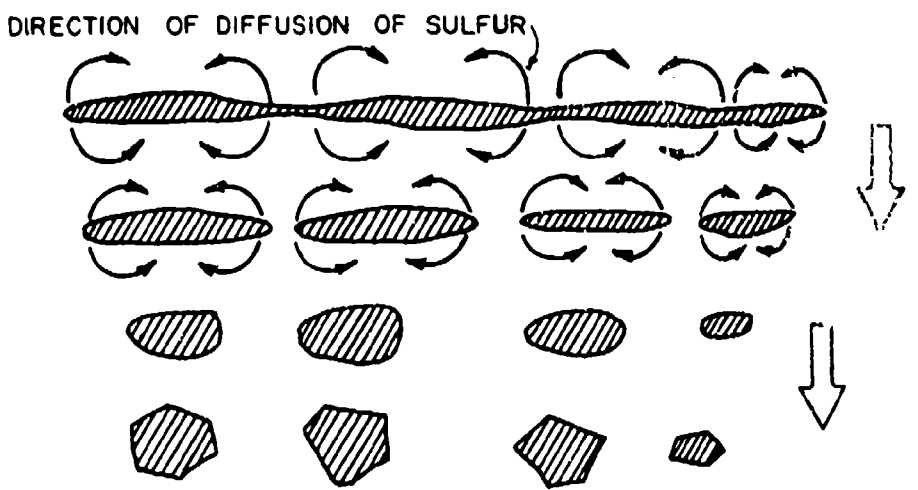


Figure 34. Geometric transformation of elongated sulfide inclusions during homogenization of hot-rolled AISI 4340 low alloy steel. Schematic representation.

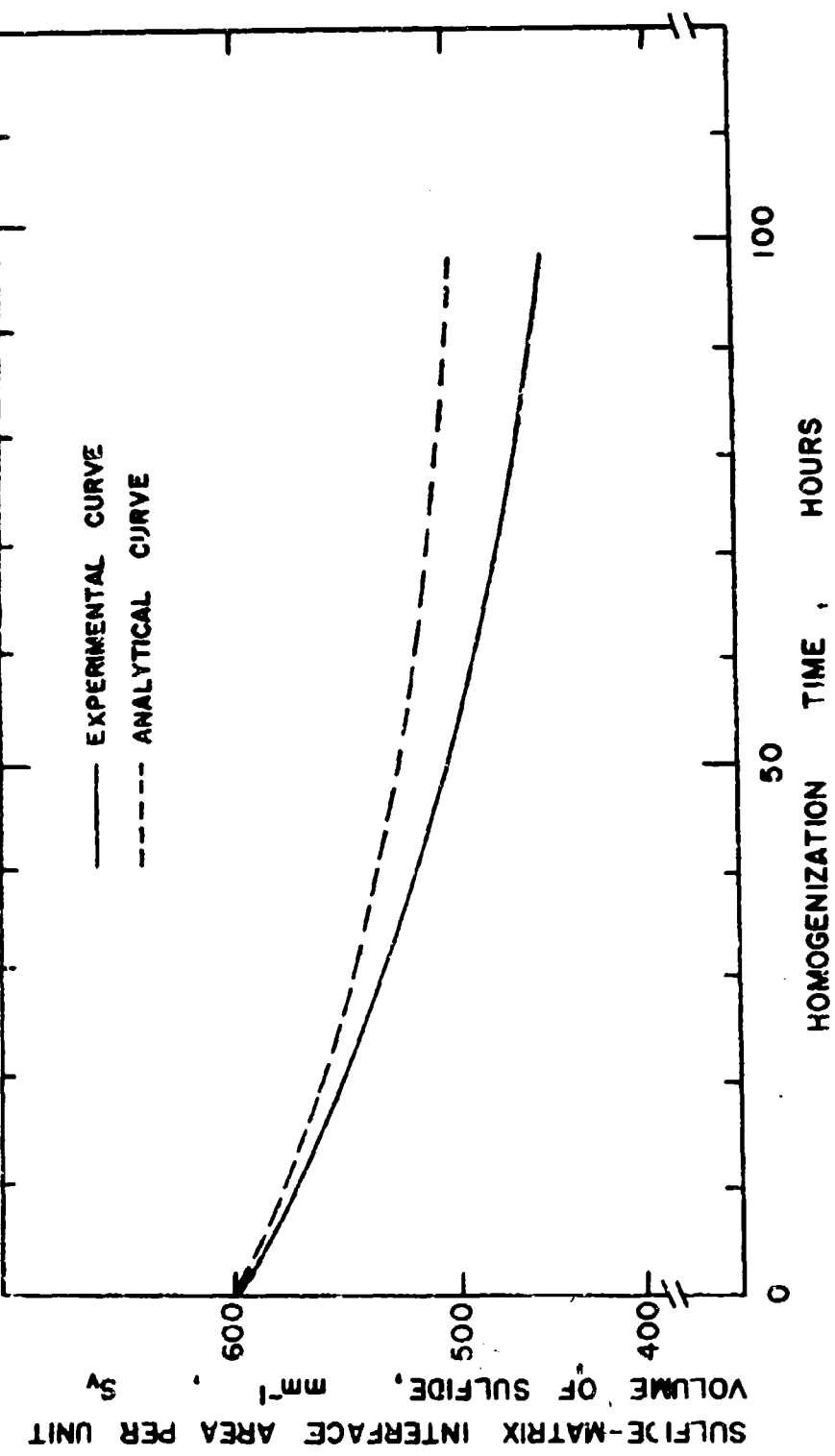


Figure 35. Variation of S with homogenization time for inclusions in specimens taken at 0.50 inches from the chill. Analytical and experimental curves. AISI 4340 unidirectionally solidified low alloy steel. Cast material.